

University of Alberta

Characterization of Arf4•GDP

by

Nathan Summerfeldt

A thesis submitted to the Faculty of Graduate Studies and Research
in partial fulfillment of the requirements for the degree of

Master of Science

Department of Cell Biology

©Nathan Summerfeldt

Fall 2010

Edmonton, Alberta

Permission is hereby granted to the University of Alberta Libraries to reproduce single copies of this thesis and to lend or sell such copies for private, scholarly or scientific research purposes only. Where the thesis is converted to, or otherwise made available in digital form, the University of Alberta will advise potential users of the thesis of these terms.

The author reserves all other publication and other rights in association with the copyright in the thesis and, except as herein before provided, neither the thesis nor any substantial portion thereof may be printed or otherwise reproduced in any material form whatsoever without the author's prior written permission.

Examining Committee

Dr. Paul Melançon, Department of Cell Biology

Dr. Paul LaPointe, Department of Cell Biology

Dr. Thomas Simmen, Department of Cell Biology

Dr. Mark Glover, Department of Biochemistry

Abstract

In this thesis, I characterized the association of Arf4•GDP with ER-Golgi intermediate compartment membranes. We confirmed that GDP-arrested Arf4 mutants associated with membranes irrespective of nature of tag or mutation. Recruitment appeared specific since loss of N-terminal myristoylation abolished binding. Surprisingly, mutations of residues unique to class II Arfs did not prevent recruitment of Arf4 to peripheral puncta. We then examined the failure of the GDP-arrested Arf4 mutant to disrupt Golgi structure. We identified residues R⁷⁹ and E¹¹³ (likely involved in salt bridge interaction) only present in Arf1 and Arf5 as critical to the ability of their GDP-arrested mutants to disrupt Golgi structure. As predicted, introduction of these residues transformed Arf4•GDP into a dominant negative mutant. Interestingly, overexpression of the putative Arf•GDP receptor membrin prevented the effects of dominant negative Arf1 but not dominant negative Arf4. These results will facilitate identification of a novel Arf target critical to protein trafficking.

Acknowledgements

Most importantly, I would like to thank my supervisor Dr. Paul Melançon for accepting me into his lab and training me. His guidance, patience, and support have opened up my eyes to the world of research. I would also like to thank my committee members, Dr. Thomas Simmen and Dr. Paul LaPoine, for their helpful discussion and guidance, and for staying awake during my long committee meetings. I would like to thank Dr. Paul LaPointe for all of his time outside the committee meetings in helping me optimize my experiments. I would also like to thank Dr. Mark Glover for agreeing to sit on my committee.

I would like to thank past and present members of the lab including Dr. Justin Chun especially for training me in the beginning of my studies, Dr. Florin Manolea, Doug, Ian, Heber, and David. Lastly, I would like to thank my family and friends for their support throughout the years.

Table of Contents

CHAPTER ONE: INTRODUCTION	1
1.1 General overview of the secretory pathway	2
1.2 Early secretory trafficking by COPII	2
1.3 Characterization and sorting at ERGIC	4
1.4 Post ER cargo trafficking by COPI	5
1.5 SNARE targeting	6
1.6 Members of the p24 protein family	7
1.7 Arf classes and localization	9
1.8 Arf GEFs	11
1.9 Arf GAPs	13
1.10 Structural aspects of Arf1	14
1.11 Characterization of Arf4	16
1.12 Mutants to uncover Arf function	18
1.13 Arf•GDP receptors	19
1.14 Rationale for thesis	22
CHAPTER TWO: MATERIALS AND METHODS	23
2.1 Reagents	24
2.2 Antibodies	29
2.3 Cell culture	30
2.4 Construction of plasmids	31
2.4.1 Arf dominant negative and constitutively active proteins tagged with Green Fluorescence Protein (GFP) and or the haemagglutinin (HA) epitope	31
2.4.2 Arf4 G2A tagged with HA and Arf4 T31N G2A tagged with GFP	32
2.4.3 Arf4 T31N chimeras tagged with GFP	32
2.4.4 Arf T31N bridge mutants	34
2.5 Plating and transient transfection of cells	39
2.6 siRNA knock down	39
2.7 Immuno fluorescence	39
2.8 Fluorescence microscopy	40
2.8.1 Epifluorescence microscopy	40
2.8.2 Live cell imaging microscopy	40
2.9 Cell lysis, fractionation and preparation of cell extracts	41
2.10 SDS Polyacrylamide gel electrophoresis (SDS-PAGE)	42
2.11 Immunoblotting	42
2.12 Quantitation of Arf release kinetics	43
CHAPTER THREE: RESULTS	45
3.1 Dominant negative versions of Arf4 are retained at puncta	46

3.2 Arf4 siRNA knock down has no impact on Golgi complex integrity	50
3.3 Myristoylation is required for association of Arf4•GDP mutants with ERGIC membranes	53
3.4 Four early secretory SNAREs unlikely to recruit Arf4•GDP at ERGIC	57
3.5 Identifying residues in Arf4 may be important to target ERGIC	62
3.6 Residues that may play an important role in dominant negative behaviour in Arf1 T31N	67
3.7 Dominant negative behaviour appears as a result from interacting with a protein other than membrin	78
 CHAPTER FOUR: DISCUSSION	 83
4.1 Summary	84
4.2 Identifying Arf4 function	85
4.3 Arf4, a role at the ER?	87
4.4 Arf4 recruitment to ERGIC	88
4.5 Impact of BFA, Golgicide (GCA) , and T31N mutant on VSVG and ERGIC	90
4.6 Mechanism for dominant negative effect of “GDP arrested” Arf mutants	91
4.7 Arf4•GDP receptor	92
 CHAPTER FIVE: REFERENCES	 94

List of Tables

Table 2.1.1 Name and source of chemicals and reagents	24
Table 2.1.2 Commercial kits	27
Table 2.1.3 Commonly used buffers and solutions	27
Table 2.2.1 Primary antibodies used in IF	29
Table 2.2.2 Primary antibodies used in immunoblotting	30
Table 2.4.1 Summary of Arf4 T31N chimera's obtained	33
Table 2.4.2 Arf bridge mutants constructed	34
Table 2.4.3 Primers used for molecular cloning	35
Table 3.1 Arf1 and 4 mutants effects on the Golgi complex	74

List of Figures

Figure 1.1 Arf GTPase cycle	10
Figure 1.2 Conformation change from Arf1•GDP to Arf1•GTP	15
Figure 1.3 Threonine plays an important role in binding β -phosphate as well as Mg^{2+} ion	20
Figure 3.1 GDP arrested mutants of Arf4 associate with peripheral puncta irrespective of the nature of tag or mutation	47
Figure 3.2 BFA treatment causes dissociation of both Arf1 and Arf4 even in BGMK cells	49
Figure 3.3 Treatment with siRNAs effectively reduces exogenous Arf4-GFP expression	51
Figure 3.4 The Golgi complex remains intact after treatment with Arf4 targeted siRNAs	52
Figure 3.5 Myristoylation at glycine 2 of Arf4 is required for membrane binding	55
Figure 3.6 Subcellular fractionation confirms importance of myristoylation in membrane binding	56
Figure 3.7 Localization of early secretory SNAREs	58
Figure 3.8 Membrin over-expression alters the distribution of Arf1 T31N	60
Figure 3.9 None of the early secretory SNAREs alter the localization of Arf4 T31N	61
Figure 3.10 Alignment of the sequences of Arf1, 4, and 5 identifies 17 residues conserved in Arf4 and 5 but divergent in Arf1	63
Figure 3.11 Arf4 T31N remains puncta bound in the absence of a Golgi complex	65
Figure 3.12 Arf4 T31N chimeras remain puncta bound	66
Figure 3.13 Arf1 and 5 T31N disrupt the Golgi complex whereas Arf4 T31N does not	69
Figure 3.14 5 residues unique to Arf1 and 5 that may determine whether the T31N mutation yields a dominant negative	70
Figure 3.15 Introduction of bridge residues R^{79} and E^{113} into Arf4 T31N-GFP yields a dominant negative mutant	71
Figure 3.16 Disruption of putative bridge between residues R^{79} and E^{113} in Arf1 T31N-GFP reduces dominant negative effect	73
Figure 3.17 Bridge residues R^{79} E^{113} are important for dominant negative behaviour	75
Figure 3.18 β COP staining confirms dominant negative phenotype	76
Figure 3.19 Myc-membrin over-expression traps Arf1 T31N in an inactive conformation at the Golgi complex	80
Figure 3.20 Over-expression of myc-membrin fails to rescue the dominant negative effect of Arf4 T31N K79R V113E	81

Abbreviations

A	alanine
Arf	ADP-Ribosylation factor
ARNO	Arf-nucleotide binding site opener
BFA	brefeldin A
BRAG	Brefeldin resistant Arf GEF
C	cysteine
COP	coatomer protein
D	aspartate
E	glutamate
ER	endoplasmic reticulum
ERES	ER exit sites
ERGIC	ER-Golgi intermediate compartment
FBS	fetal bovine serum
GAP	GTPase activating protein
GBF1	Golgi BFA resistant factor 1
GDP	guanine diphosphate
GEF	guanine nucleotide exchange factor
GFP	green fluorescent protein
GTP	guanine triphosphate
H	histidine
HA	hemagglutinin
I	isoleucine
IF	immunofluorescence
IP	immunoprecipitation
K	lysine
L	leucine
M	methionine
Mg ²⁺	magnesium
N	asparagines
NA	numerical aperture
PM	plasma membrane
Q	glutamine
R	arginine
S	serine
SDS-PAGE	sodium dodecyl sulphate-polyacrylamide gel electrophoresis
SNARE	soluble N-ethylmaleimide-sensitive factor attachment protein
T	threonine
TGN	<i>trans</i> -Golgi network
VSVG	vesicular stomatitis viral G protein
VTC	vesicular tubular cluster
w/v	weight per volume

CHAPTER ONE: INTRODUCTION

1.1 General overview of the secretory pathway

The Golgi complex, the elaborate central sorting station of the secretory pathway, displays a complex structure to facilitate trafficking and sorting of cargo molecules (Mogelsvang et al., 2004; Rambourg and Clermont, 1990). The Golgi complex appears as a ribbon structure comprised of a collection of highly fenestrated cisternae. From **ER exit sites** (ERES), cargo shuttles towards **vesicular tubular clusters** (VTCs) alternately called the **Endoplasmic Reticulum Golgi Intermediate Compartment** (ERGIC) (Fromme and Schekman, 2005; Tang et al., 2005). The ERGIC functions as the first post-ER sorting station from which cargo traffics in either an anterograde direction to the Golgi complex or returns in a retrograde direction to the ER (Appenzeller et al., 1999). At the Golgi complex, carriers combine to form a network and transform into *cis*-Golgi cisternae (Bonifacino and Glick, 2004). In one accepted model, it is thought that cargo, once transferred to *cis*-Golgi cistern, remains in that cisterna as it progresses through the Golgi stack and undergoes a process of cisternal maturation. The cargo-containing cisternae lose early acting enzymes and acquire late acting enzymes as they move from a *cis*- to a *trans*- position in the Golgi (Losev et al., 2006; Matsuura-Tokita et al., 2006; Puthenveedu and Linstedt, 2005). Once cargo reaches the *trans*-Golgi network (TGN), it faces a number of possible destinations, namely the endosome, **plasma membrane** (PM), secretory granules, or lysosomes (Rodriguez-Boulan and Musch, 2005).

1.2 Early secretory trafficking by COPII

Cargo is initially shipped from the ER to either the ERGIC or Golgi complex in COPII coated vesicles. COPII assembly initiates at ERES in most eukaryotes (Orci et al., 1991). The GTPase Sar1 recruits the coat proteins that make up the COPII coat (Nakano and Muramatsu, 1989). Sec12, an ER-bound regulator is responsible for activating Sar1 (Barlowe and Scheckman, 1993). Activated Sar1 recruits the Sec23-Sec24 heterodimer by binding the Sec23 subunit (Sato and Nakano, 2007). This complex then further recruits the outer coat tetramer Sec13-Sec31 (Lederkremer et al., 2001). The COPII structure was solved to reveal a tetrameric assembly of the Sec23-Sec24 component below the Sec13-Sec31 lattice component (Stagg et al., 2008). The three subunits, Sar1, Sec23-24, and Sec13-31 are sufficient to drive vesicle formation on liposomes (Matsuoka et al., 1998). It has been suggested that the outer layer drives membrane deformation resulting in vesicle formation (Sato and Nakano, 2007). Additionally, it has been shown that sec16 may function as a scaffolding protein in COPII vesicles (Connerly et al., 2005; Espenshade et al., 1995).

Sar1 like most GTPases is inactivated by a GAP, which in this case is the Sec23 subunit of COPII; interestingly interaction with Sec13-Sec31 enhances the Sec23 GAP activity (Antonny et al., 2001). It could be that the kinetics of vesicle budding are faster than GTP hydrolysis of Sar1 or that even with Sar1 inactivation and release from membranes, the assembled Sec23-Sec24/Sec13-Sec31 complex is sufficient to drive vesicle formation (Bonifacino and Glick, 2004). Trans-membrane proteins are selected into COPII vesicles by direct interaction

between the COP components and export signals on the cargo protein (Sato and Nakano, 2007). For example, VSVG has a di-acidic (D/ExD/E) export signal (Nishimura and Balch, 1997) whereas ERGIC-53 has two phenylalanines at the C-terminus important for efficient export from the ER (Kappeler et al., 1997). The COPII components shown to bind cargo are Sec24 and Sar1. Sec24 has been shown to have three signal binding sites that recognize different export signals (Mancias and Goldberg, 2008; Miller et al., 2003).

1.3 Characterization and sorting at ERGIC

The ERGIC is a membranous structure found in between the ER and Golgi complex (Appenzeller-Herzog and Hauri, 2006). There has been a significant amount of work in developing two models to understand ERGIC's role in ER to Golgi traffic. Live cell imaging of a well characterized GFP tagged cargo marker, Vesicular Stomatitis Virus G protein (VSVG) first suggested that ERGIC functions as a motile transport intermediate between the ER to the Golgi (Presley et al., 1997). This initial model, called the transport complex model, suggested that ERGIC itself was mobile and formed from COPII derived vesicles that migrated on microtubules and eventually fused with *cis*-Golgi elements (Appenzeller-Herzog and Hauri, 2006). Further work with additional markers demonstrated that this model was not accurate. For example, live cell microscopy with ERGIC-53-GFP revealed static structures from which tagged cargo proteins are shuttled out (Ben-Tekaya et al., 2005). These results suggest that ERGIC acts as a stable compartment rather than a transient compartment.

The mannose-specific membrane lectin protein, ERGIC-53, was the first protein identified to define ERGIC (Hauri et al., 2000; Schweizer et al., 1988). More recently, two other ERGIC-restricted proteins have been described, Surf4 and p25 both of which have been implicated in maintaining the integrity of the ERGIC (Mitrovic et al., 2008). p115, a peripheral membrane protein localized to the Golgi complex (Waters et al., 1992) as well as at the ERGIC (Nelson et al., 1998) has a role in translocating ERGIC vesicles to the Golgi complex (Alvarez et al., 1999). Yip1A, a transmembrane protein from a family of proteins that regulate rab membrane recruitment, has also been found at ERGIC (Kano et al., 2009; Yoshida et al., 2008); however, it may function to recruit the Golgi localized Rab6 (Kano et al., 2009). Rab1 has been shown to have a role at ERGIC where it may help regulate traffic that bypasses the Golgi by forming connections with the centrosome (Marie et al., 2009). Rab1 studies reveal ERGIC not only as a way station in cargo sorting from the ER to the Golgi complex but as an independent site for Golgi independent trafficking (Saraste et al., 2009). Rab2 as well has been implicated to function at the ERGIC where it recruits β COP (Tisdale and Jackson, 1998).

1.4 Post ER cargo trafficking by COPI

COPI vesicles are implicated in retrograde traffic from the ERGIC to the ER as well as in intra-Golgi transport (Béthune et al., 2006). To complicate matters, current evidence supports two conflicting models of intra-Golgi trafficking by

COPI. The cisternal/maturation model proposes that *cis*-cisternae mature as they progress through the Golgi stack where upon reaching the *trans*-side they would disassemble. Anterograde cargo would not require COPI vesicle formation as it would move with the maturing cisternae. In this model, COPI vesicles transport Golgi resident enzymes from later cisternae to earlier ones (Glick and Malhotra, 1998). In contrast, the vesicle transport model proposes that COPI vesicle transport cargo in both anterograde and retrograde directions as cisternae remain static (Béthune et al., 2006). The COPI coat consist of 7 subunits, α -, β -, γ -, δ -, β' -, ϵ -, and ζ -COP and unlike COPII, appears to form *en bloc* (Hara-Kuge et al., 1994). Arf1 recruits COPI through the β - and γ -coat subunits (Zhao et al., 1997; Zhao et al., 1999). In parallel, COP1 coats also bind trans-membrane proteins bearing a di-lysine motif (Cosson and Letourneur, 1994) that may strengthen the Arf1-COPI interaction (Bremser et al., 1999).

1.5 SNARE targeting

SNAREs or soluble N-ethylmaleimide-sensitive factor attachment protein receptors are involved in the final stage of vesicle trafficking, docking and fusion of the donor vesicle to the acceptor membrane. They are relatively small proteins of 100-300 amino acids, containing an evolutionary conserved SNARE domain (Hong, 2005). SNAREs can be classified based on functionality (v-SNAREs and t-SNAREs) or structure (S and Q SNAREs) (Hong, 2005). A v-SNARE present on a vesicle will interact with a t-SNARE trimer complex found on target membranes that will lead to membrane fusion (Weber et al., 1998). A single v-SNARE

interacts with the three t-SNAREs by forming a twisted parallel four helical bundle called a SNAREpin (Sutton et al., 1998). Classification based on structure uses the highly conserved SNARE domain and categorizes based upon presence of an S or Q residue within the SNARE domain (Fasshauer et al., 1998). Q SNAREs can be further divided into three sub categories, called Qa, Qb, and Qc (Hong, 2005). Of the 36 known SNAREs in mammalian cells, Rbet1, Sec22b, syntaxin 5, and membrin show distribution patterns within the early secretory pathway (Hay et al., 1998). Their distribution overlaps with each other; however, Sec22b localizes mainly to the ER and ERGIC whereas syntaxin 5, membrin, and Rbet1 localize primarily to the ERGIC and *cis*-Golgi (Hay et al., 1996). It was shown that syntaxin 5 may bind each of the three other SNAREs, whereas combinations of Sec22b, Rbet1 or membrin failed to form complexes (Hay et al., 1998). SNAREs may also act as Arf•GDP receptors, which will be discussed later in section 1.13.

1.6 Members of the p24 protein family

Members of the p24 family are Type 1 trans-membrane 24 kD proteins involved in bidirectional trafficking at the ER-Golgi interface that can be divided into four subfamilies (p24 α , β , γ , and δ) (Strating and Martens, 2009). All p24 proteins share the following conserved domain architecture: N-terminal GOLD (**G**olgi **d**ynamics) domain containing a disulfide bridge (Anantharaman and Aravind, 2002), coiled-coil region, membrane spanning domain, short cytoplasmic tail with a conserved motif to target COP1 and COPII (Strating and Martens, 2009). Depending on their localization, the p24s are thought to

function as either monomers, or dimers (Jenne et al., 2002) formed through their coiled-coil domains (Ciufo and Boyd, 2000). They have been associated with both COPI and COPII vesicles at the ER, ERGIC, and *cis*-Golgi (Strating and Martens, 2009). Surprisingly, yeast studies have shown that a strain in which all members of the p24 family have been knocked out remained viable, with only minor secretory pathway defects (Springer et al., 2000). However, in multicellular organisms a more complex scenario must exist since mouse studies have shown that knock out of p24 δ_1 resulted in embryonic lethality (Denzel et al., 2000).

Members of the p24 family have been shown to perform various roles. They were first thought to function as cargo receptors (Stamnes et al., 1995) since inhibition of p24s by antibody injection caused accumulation of the cargo VSVG at ERGIC (Rojo et al., 1997). p24 members have also been shown to be important in the formation of COPI vesicles (Bethune et al., 2006) by either binding Arf1•GDP and coatamer complex, or by binding Arf GAP1 to block its activation (Goldberg, 2000). The p24 members have also been shown to participate in organization of the ER and Golgi membranes (Strating and Martens, 2009). Over-expression of p23/p24 δ_1 or p24/p24 β_1 results in expanded ER membranes and fragmented Golgi membranes (Blum et al., 1999). All together, these observations hint towards a role in early secretion; however, much work is needed to understand the overall mechanism of p24 family of proteins.

1.7 Arf classes and localization

Arfs or **A**DP-**r**ibosylation **f**actors are small GTPases that regulate a wide variety of effectors, including coat proteins and lipid remodelling enzymes. They are themselves regulated by **G**uanine **N**ucleotide **E**xchange **F**actors (GEFs) and **G**TPase **A**ctivating **P**roteins (GAPs) (Fig 1.1). The 21 kDa proteins are structurally and functionally conserved proteins part of the Ras superfamily of regulatory GTP binding proteins (Boman and Kahn, 1995). GEFs activate Arfs by promoting the dissociation of GDP whereas GAPs inactivate Arfs by enhancing their GTP hydrolysis rate. Not only have they been described at the Golgi complex but also at the ER, the nuclear envelope, membranes of the endocytic pathway, early endosomes and at the plasma membrane (Boman and Kahn, 1995). They function primarily in membrane traffic through regulation of cytosolic coat proteins (Bonifacino and Lippincott-Schwartz, 2003). Arfs can also activate PLD, an enzyme responsible for hydrolyzing phosphatidylcholine to phosphatidic acid and choline (Boman and Kahn, 1995), as well as recruit the lipid kinase PI4K β (De Matteis et al., 2002).

There are six mammalian Arf isoforms (Cavenagh et al., 1996). The six Arfs are grouped by sequence similarity into 3 categories, class one (Arf1, 2 and 3), class two (includes Arfs 4 and 5) and class three (Arf6) (Cavenagh et al., 1996). Of the class one Arfs, human cells express only Arf1 and Arf3. Class one Arfs show 96% identity with one another whereas class two display 90% identity with one another and 81% identity with Arf1. Lastly, Arf6, the most unique of the six, displays only 66-70% identity to the other classes (Cavenagh et al., 1996). Arf1 is

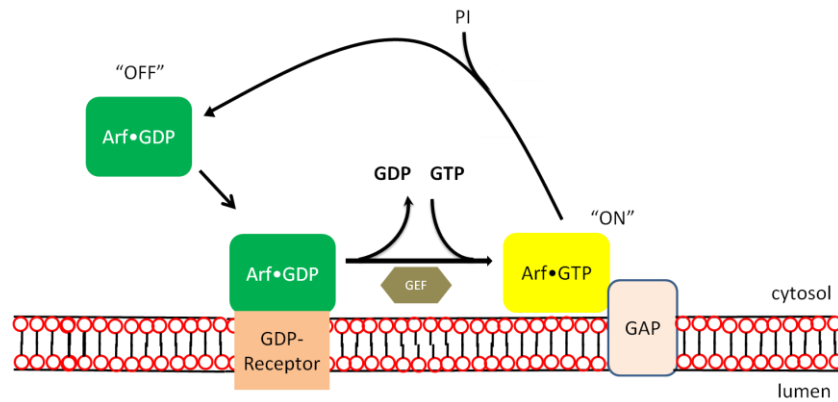


Figure 1.1 General Arf GTPase cycle

Soluble Arf•GDP is recruited to the membrane by an Arf•GDP-receptor. A guanine nucleotide exchange factor (GEF) promotes the dissociation of GDP and association of GTP on Arf, resulting in Arf activation. A GTPase activating protein (GAP) inactivates by promoting the intrinsic hydrolysis of GTP to GDP.

involved in the ER-Golgi system where it mediates traffic and regulates coat protein recruitment (Lippincott-Schwartz and Liu, 2003) whereas Arf6 is found to regulate endocytic cargo at the plasma membrane (D'Souza-Schorey et al., 1995). Arf3 may also function at restricted sites in the cell as it has been recently shown to localize primarily at the *trans*-Golgi (Manolea et al., 2010).

1.8 Arf GEFs

As mentioned before, GEFs are required to facilitate activation of Arfs, and like Arfs there are a variety of GEFs. All Arf GEFs possess a conserved 200 amino acid Sec7 domain, responsible for GEF activity. There are five families of eukaryotic GEFs classified based upon domain organization and overall structure: **G**olgi **B**FA-resistant **f**actor 1/**B**FA inhibited **G**EF (GBF/BIG), **A**rf **n**ucleotide binding site **o**penner (ARNO)/cytohesin, **e**xchange **f**actor for **A**rf**6** (EFA6), **B**refeldin **r**esistant **A**rf **G**EF (BRAG) and **F**-**b**ox only protein (FBX8) (Casanova, 2007). Cytohesins are the best characterized Arf GEFs. They predominantly localize to the cell periphery (Frank et al., 1998) and plasma membrane in response to PI3 kinase signalling (Klarlund et al., 1997). Recruitment to the plasma membrane may also be regulated by an interaction of Arf6 with the PH domain of ARNO (Cohen et al., 2007). These authors further showed that ARNO although it interacts with Arf6, preferentially activates Arf1 *in vivo*.

The EFA6 brain specific Arf GEFs, like the cytohesins, localize to the plasma membrane (Derrien et al., 2002) and activate only Arf6 even *in vitro* (Luton et al.,

2004). The BRAGs are BFA resistant Arf GEFs found primarily in neuronal tissue (Casanova, 2007). They also function in non-neuronal cells where they activate Arf6, regulating endocytosis but unlike the cytohesins and EFA6s, are insensitive to phosphoinositide regulation (Casanova, 2007). Little is known about the FBX8 Arf GEFs but that they form multi-subunit ubiquitin-ligase complexes that may function to degrade Arfs by ubiquitination or perhaps activate Arfs by active protein ubiquitination (Casanova, 2007).

The GBF/BIG family contains GBF1, BIG1, and BIG2 that are responsible for activating class 1 and class 2 Arfs (Casanova, 2007). Both GEFs are sensitive to a small fungal heterocyclic lactone called BFA that induces Golgi breakdown and causes a recycling of Golgi resident enzymes to the ER (Donaldson et al., 1992; Pelham, 1991). Overexpression of GBF1 protects cells against BFA; however, endogenous GBF1 is BFA sensitive. Anterograde traffic from the ER to the Golgi is blocked after BFA addition (Lippincott-Schwartz et al., 1989). It is well documented that BFA targets the sec7 domain of Arf-GEFs, the catalytic domain responsible for exchange of GDP for GTP on Arf, preventing its activation (Mansour et al., 1999; Mossessova et al., 2003; Peyroche et al., 1999; Robineau et al., 2000). Crystallography studies show that BFA binds in a hydrophobic groove created at the interface between the Sec7 domain and the Arf•GDP (Renault et al., 2003; Zeghouf et al., 2005). GBF1 is found primarily at the ERGIC and *cis*-Golgi (Zhao et al., 2006) whereas BIGs 1 and 2 localize primarily at the TGN (Zhao et al., 2002) and at perinuclear endosomes (Shin et al., 2004). GBF1

can directly recruit COP1 coat independently of Arf activation (Deng et al., 2009), whereas BIGs indirectly recruit AP-1 and GGA's (Casanova, 2007). Our lab demonstrated that GBF1 functions primarily at the *cis*-Golgi whereas BIGs function primarily at the *trans*-Golgi (Manolea et al., 2008). Arf activation at ERGIC, the topic of this thesis, would therefore most likely involve GBF1 and not BIGs 1 or 2.

1.9 Arf GAPs

Arf GAPs not only inactivate Arfs by promoting GTP hydrolysis but also provide structural support to transport intermediates independent of Arfs (Yang et al., 2002). 15 Arf GAPs containing a conserved Arf GAP domain have been identified that can be divided based on their overall domain structure (Randazzo and Hirsch, 2004). Like the GEFs, Arf GAPs show some specificity towards Arf-GTP substrates. Arf GAP1 and Arf GAP2 preferentially use Arf1 as substrate *in vitro* (Randazzo, 1997). *In vivo* work found the KDEL receptor to recruit Arf GAP to the membrane where it reduced the amount of active Arf1 (Aoe et al., 1997). AGAP1 has also been shown to interact with Arf1 but at sites different from where Arf GAP1 and 2 function (Randazzo and Hirsch, 2004). Arf6 preferentially acts as a substrate and associates with ACAP1 and ACAP2 by co-localization at the cell periphery (Jackson et al., 2000). *In vitro* work suggests that a subtype of Arf GAP1, the **G** protein-coupled receptor kinase interactors (Gits) act promiscuously on all Arfs; however, *in vivo* work found Gits to localize only to the

cell periphery where Arf6 predominantly localizes (Randazzo and Hirsch, 2004). The known Arf GAPs for class 2 Arfs remain poorly characterized. ASAP1 and ASAP2 have been shown to preferentially recruit Arf5 as substrate over Arf1 and Arf6 (Randazzo and Hirsch, 2004). In contrast, ASAP1 has been implicated to act on Arf1 and Arf6. Clearly, more research is required to understand class 2 Arf inactivation.

1.10 Structural aspects of Arf1

Crystallography experiments have helped unveil the structural changes and steps needed for Arf activation (Pasqualato et al., 2002). Arf1 activation/inactivation cycling occurs by a mechanism that incorporates the interswitch (switch1 and switch 2), and the myristoylated N-terminal amphipathic helix that normally docks onto a hydrophobic groove on the Arf surface (Figure 1.2) (Pasqualato et al., 2002). Once Arf1•GDP approaches membranes, the N-terminal helix will extend from the hydrophobic groove and insert weakly into the membrane (Cherfils and Melançon, 2005). Analysis of the X-ray structures of GDP and GTP-bound form of Arf1 revealed that exchange of GDP for GTP causes both switch 1 and 2 to shift allowing the interswitch to occupy the hydrophobic groove, forcing the N-terminal helix to remain membrane imbedded (Goldberg, 1998). Subsequent work with intermediates arrested with either BFA or point mutants of the Sec7 domain have provided 3D snapshots on the mechanism of Arf activation by the GEF. First, the Sec7 domain.

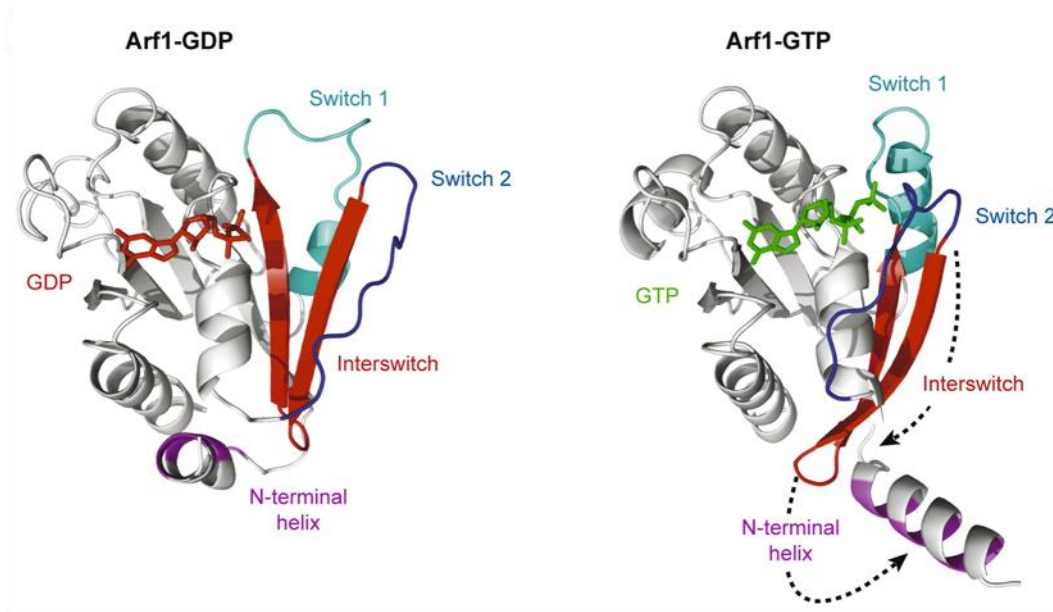


Figure 1.2 Conformational change from Arf1•GDP to Arf1•GTP

Arf1 bound to either GTP or GDP contains the switch 1 (blue), switch 2 (dark blue), interswitch (red), and the N-terminal helix (purple). In a GTP bound state, the interswitch of Arf1 shifts relative to switch 1 and 2 towards the hydrophobic groove. The N-terminal helix is unable to retract back to its hydrophobic groove and remains extended in an active conformation that interacts with lipid bilayer membranes. Adapted from Gillingham and Munro, 2007.

appears to bind Arf•GDP before the N-terminus is extended from the N-terminus groove, suggestive that Arf-GEF binding could occur in cytosol (Cherfils and Melançon, 2005). Subsequently, a glutamate in the sec7 domain disrupts the Mg^{2+} and phosphate groups in the GTP binding site of Arf, thereby promoting GDP expulsion (Goldberg, 1998).

1.11 Characterization of Arf4

Arf4 has been shown to have a specific function in photoreceptor cells where it binds the C terminus of rhodopsin and regulates its packaging into rhodopsin transport carriers destined for the rod outer segment (Deretic et al., 2005). This trafficking complex not only included rhodopsin and Arf4, but also Rab11 and FIP3 (Mazelova et al., 2009). Arf4 was found to target specifically the VxPx motif of rhodopsin and this interaction was found to be specific to Arf4 through its α 3 helix (Mazelova et al., 2009).

Little is known about the general cellular function of Class II Arfs, but recent work from our lab has shed new light. It was established that when cells were treated with BFA Class II Arfs quickly released from the Golgi but remained on peripheral ERGIC puncta, likely in a GDP-bound state (Chun et al., 2008). This was confirmed using a dominant negative mutant of Arf4 favoured in its GDP state that accumulated on ERGIC-53 positive structures and clearly not at the Golgi (Chun et al., 2008). Subsequent live cell imaging studies revealed that Arf4-GDP association with ERGIC did not involve the predicted Arf-GEF complex formed

upon BFA treatment since Arf4 could be readily separated from GBF1 (Chun et al., 2008). These results suggest the presence of a receptor specific for Arf4 at the ERGIC (Chun et al., 2008). Contrary to the clear release of class II Arfs from the Golgi reported by Chun *et al.*(2008), Daniël et al. (2009) reported that Arf4 but not Arf1 remained associated with the Golgi complex in BGMK cells after 5 minutes of BFA treatment (Daniël et al., 2009). The authors identified residues at the N terminus and in the interswitch domain as responsible for this differential binding of Arf4 and Arf1 (Daniël et al., 2009).

Although knock down of a single Arf yielded no impact on the secretory pathway, double KD of varying combinations of Arf did (Volpicelli-Daley et al., 2005). One of the more striking experiments revealed that double knock down of Arf1 and 4 redistributed the peripheral cytoplasmic *cis*-Golgi protein GM130 (Nakamura et al., 1995) into puncta and cytosol, dispersed the integral Golgi membrane protein giantin (Linstedt and Hauri, 1993) into small puncta, and retained most cargo protein (VSVG) at the ER (Volpicelli-Daley et al., 2005). These results hint that perhaps Arf4 has a unique function at ERGIC.

1.12 Mutants to uncover Arf function

Dominant mutant proteins have been widely used as tools to probe biological processes. Several useful Arf mutants were developed on the basis of well-characterized Ras mutants (Lowy and Willumsen, 1993) as they share conserved GTP binding pockets (Bourne *et al.*, 1991). Several mutants that arrest

in the GDP-bound state were originally selected following random mutagenesis of Ras (Feig and Cooper, 1988). Mutation S17N in Ras has been shown to alter the nucleotide binding affinity resulting in a favored GDP-bound form (Feig and Cooper, 1988), whereas mutation N116I causes limited affinity for GTP and GDP resulting in fast nucleotide cycling (Chein-Fuang and Nin-Nin, 2000). Arf T31N and N126I mutants were based on Ras mutations, S17N and N116I, respectively. Arf dominant negative mutants remain poorly characterized. Early experiments confirmed that Arf1-T31N bound GTP poorly and revealed that exogenous expression triggered a BFA like effect, where cargo export from the ER was blocked and the Golgi complex collapsed into the ER (Dascher and Balch, 1994). Over-expression of Arf1 N126I in mammalian cells induces a similar collapse of the Golgi (Holloway et al., 2007), whereas in yeast cells, Arf1 N126I expression is lethal (Zhang et al., 1994).

By examining the ``GDP-arrested`` dominant negative mutants in more detail, we can tease apart their molecular mechanism. Recent crystallography of Ras S17N confirmed that indeed this mutant protein is bound to GDP (Nassar et al., 2010). It is thought that the S to N mutation disrupts the Mg^{2+} interaction with Ras. Without Mg^{2+} , the negatively charged phosphates of GTP or GDP cannot be shielded thereby lowering the affinity of Ras for both nucleotides. The S17N mutation only reduces the affinity for GDP by a factor of 27 whereas it reduces the affinity for GTP by a factor of 1000 (Cool et al., 1999). Loss of Mg^{2+} may have a greater impact on GTP binding than on GDP binding because the

extra negative phosphate on Ras•GTP requires more shielding (Nasser et al., 2010). The equivalent mutation in class 1 and class 2 Arfs, T31N, and class 3 Arfs, T27N are thought to behave the same way as the Ras S17N mutant. Indeed, residue T27 in Arf6 was shown to interact with the β -phosphate of the nucleotide and magnesium ion in both the GTP and GDP bound forms (Macia et al., 2004) (Figure 1.3). Additional experiments further established that Arf1-T31N bound GTP poorly and likely accumulated in the GDP-bound state (Dascher and Balch, 1994). In contrast, Arf6-T31N appears to bind both nucleotides poorly and readily aggregates (Macia et al., 2004).

1.13 Arf•GDP receptors

Non-specific Arf binding to membranes occurs through the myristoylated (Palmer et al., 1993) amphipathic N-terminal helix. However, evidence suggests myristoylation is only part of the puzzle and that selective Arf recruitment to unique membranes may require a receptor. The recruitment of Arf1•GDP to the cis-Golgi provides the best example to date. Donaldson and colleagues identified a 4 residue motif, MXXE¹¹³, in Arf1 that was required to target it to the *cis*-Golgi (Honda et al., 2005). The authors developed an approach to identify a receptor responsible for targeting Arf1 by the MXXE¹¹³ motif, based on earlier work that identified SNAREs as potential candidates. Specifically, *in vitro* binding assays identified four yeast SNAREs (Bet1p, Bos1p, and Sec22p) as potential interacting partner of yeast Arf1p (Rein et al., 2002). These authors further showed that

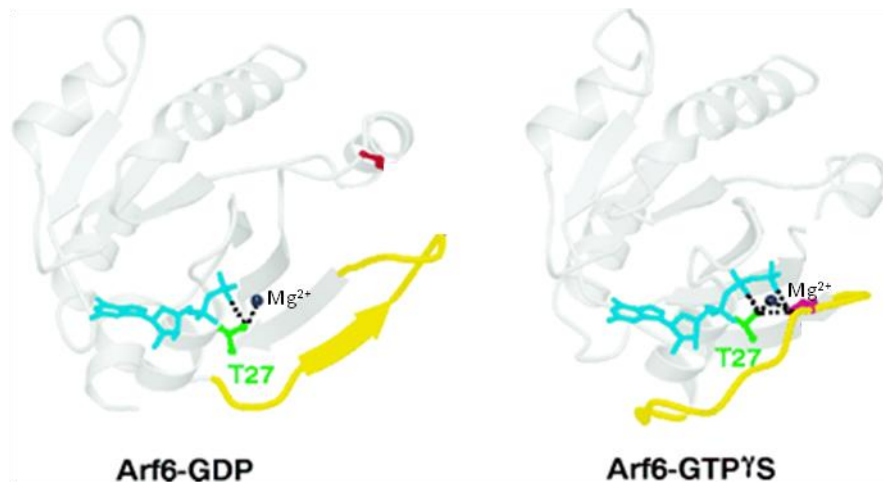


Figure 1.3 Threonine plays an important role in binding β -phosphate as well as Mg^{2+} ion.

Residue T27 (green) interacts with both nucleotide (light blue) and magnesium ion. This interaction is found in both Arf6•GDP and Arf6•GTP. Modified from Macia et al., 2004.

Arf1p bound Bet1p regardless of its nucleotide bound state (Rein et al., 2002). Using a similar approach, Honda *et al.* (2005) performed *in vitro* pull downs with His₆- tagged Arf1 following incubation in Hela cell lysates primed with GDP (Honda et al., 2005). These experiments identified membrin as a binding partner of Arf1-GDP but only after cross-linking suggesting that Arf1-GDP-membrin interaction was weak (Honda et al., 2005). Complementary experiments established that myc-membrin protected against the BFA induced redistribution of Arf1-GFP (Honda et al., 2005). In controls cells lacking over-expressed myc-membrin, BFA caused Arf inactivation, and rapid release of inactive Arf•GDP from the Golgi.

Additional proteins may be involved in the recruitment of Arf1•GDP to the Golgi complex. Indirect evidence suggests that p23, a member of the p24 family of proteins, may also function as a receptor for Arf1 (Sohn et al., 1996). *In vitro* binding assays led these authors to conclude that p23 binds the COP1 coat and potentially Arf1 since p23 amounts were stoichiometric with Arf1 and COP1 coat protein (Sohn et al., 1996). These results were extended to show a direct interaction between p23 and Arf1 at the Golgi (Majoul et al., 2001); further work showed that Arf1 interacts in a GDP bound state with the C-terminus of p23 (Gommel et al., 2001). Selective recruitment of Arf3 at the TGN may also involve a receptor specific to Arf3 (Manolea et al., 2010). Finally, Arf6•GDP-restricted mutants show a plasma membrane restricted localization, again suggestive of a unique receptor for Arf6•GDP (Macia et al., 2004).

1.14 Rationale for thesis

My thesis focused on the poorly characterized Class II Arf, Arf4. Unlike Class I Arfs, the Class II Arf, Arf4 associated with the ERGIC in a GDP conformation. We first hypothesized that both an Arf4•GDP receptor present at the ERGIC and that residues unique to Class II Arfs in Arf4 mediated this interaction. Previous observations by Dr. Justin Chun showed that not only did Arf4•GDP uniquely recruit to ERGIC but also failed to act like the Arf1 T31N and Arf5 T31N dominant negative mutants. Our second hypothesis was that Arf4 T31N must have residues unique from Arf1 and Arf5 that account for its failure to disperse the Golgi complex. We reasoned that a better understanding of why Arf4 T31N failed as a dominant negative mutant, may elucidate the mechanism through which Arf1 T31N disrupts the secretory pathway.

CHAPTER TWO: MATERIALS AND METHODS

2.1 Reagents

All use of reagents was in accordance with procedures set out by the Environmental Health and Safety of the University of Alberta and Workplace Hazardous Materials Information System (WHMIS).

Table 2.1.1 Name and source of chemicals and reagents.

Reagent	Supplier
Acetic acid, glacial	Fisher Scientific
Acrylamide/bis (30%; 29:1)	Biorad
Agarose (UltraPure™)	Invitrogen
Ammonium chloride	Caledon
Ammonium persulfate	Bio-rad
Ampicillin	Novopharm
Bactotryptone	BD
Bacto-yeast	BD
Bovine serum albumin	Sigma
Brefeldin A	Sigma
Bromophenol blue	Sigma
Calcium chloride	BDH
CO ₂ -independent medium (- L-glutamine)	Gibco (Invitrogen)
Complete, EDTA-free protease inhibitor cocktail tablets	Roche

DTT (dithiothreitol)	Fisher Scientific
DMEM (Dulbecco's Modified Eagle Medium)	Gibco (Invitrogen)
DMSO (dimethyl sulfoxide)	Sigma
dNTP (deoxyribonucleotide triphosphate)	Invitrogen
EDTA (ethylenediamine-tetraacetic acid)	Sigma
Fermentas PageRuler™ Prestained Protein Ladder Plus	Fermentas
Fetal bovine serum (FBS)	Gemini Bio-Products
Fibronectin	Sigma
Gelatin	Fisher Scientific
GeneRuler 1 kb DNA Ladder	Fermentas
Glycerol	Fisher Scientific
Glycine	Roche
hydrochloric acid	Fisher Scientific
Igepal CA-630 (NP-40)	Sigma
Isopropanol	Fisher Scientific
Kanamycin	Sigma
L-glutamine	Gibco
Magnesium chloride	BDH
Magnesium sulphate	Fisher Scientific
Methanol	Fisher Scientific
O-phenathroline	Sigma

Opti-MEM	Gibco (Invitrogen)
Paraformaldehyde	Sigma
Penicillin/streptomycin	Gibco (Invitrogen)
PBS (phosphate buffered saline; Dulbecco's)	Gibco (Invitrogen)
Phosphate-free DMEM	Invitrogen
Platinum® Pfx DNA polymerase	Invitrogen
Ponceau S	Sigma
Potassium chloride	BDH
Precision Plus protein standard	Bio-rad
Prolong® Gold with DAPI antifade reagent	Molecular Probes (Invitrogen)
Restriction endonucleases	Invitrogen or NEB
Sodium bicarbonate	Caledon
Sodium chloride	Fisher Scientific
SDS (sodium dodecyl sulfate)	Bio-rad
Sodium fluoride	Sigma
Sodium hydroxide	Fisher Scientific
Sucrose	Sigma
SYBR Safe DNA gel stain	Molecular probes (Invitrogen)
T4 DNA ligase	Invitrogen
TEMED (tetramethylethylenediamine)	OmniPur
TransIT-LTI transfection reagent	Mirus

Tris (tris-(hydroxymethyl)aminomethane)	Roche
Triton X-100	VWR
Trypsin-EDTA	Gibco (Invitrogen)
Tween 20 (Polysorbate 20)	Fisher Scientific

Table 2.1.2 Commercial Kits

Kit	Supplier
ECL Plus Western Blotting Detection System	GE Healthcare
GeneJET Plasmid miniprep kit	Fermentas
QIAGEN Plasmid Midi kit	QIAGEN
QIAprep spin miniprep kit	QIAGEN
QIAquick gel extraction kit	QIAGEN
QuickChange Site-Directed Mutagenesis Kit	Stratagene

Table 2.1.3 Commonly used buffers and solutions

Solution	Composition
Homogenization Buffer	10 mM HEPES pH 7.4, 250mM sucrose, 1mM EDTA, 1mM EGTA, o-phenanthroline, pepstatin A, and Complete Mini, EDTA-free protease inhibitor cocktail tablets (Roche)
Luria-Bertani (LB) Broth	1% bactotryptone, 0.5% bacto-yeast extract,

	1% (w/v) NaCl, pH 7.0
Lysis buffer	10mM Tris-HCL pH 8.0, 150 mM NaCl, o-phenanthroline, pepstatin A, and complete mini, EDTA-free protease inhibitor cocktail tablets (Roche)
Paraformaldehyde (3%)	3% paraformaldehyde, 0.1 mM CaCl ₂ , 0.1 mM MgCl ₂
Permeabilization buffer	0.1% (v/v) Triton X-100, 0.05% SDS in PBS
Phosphate buffered saline (PBS)	2.7 mM KCl, 1.5 mM KH ₂ PO ₄ , 137.9 mM NaCl, 8.1 mM Na ₂ HPO ₄
Quench buffer	50 mM NH ₄ Cl in PBS
Running buffer	25 mM Tris-HCl, 190 mM glycine, 0.1% SDS
SDS-PAGE sample buffer (6X)	30% (v/v) glycerol, 1% SDS, 0.6 M DTT, 0.012% bromophenol blue, 70% (v/v) 4X Tris-HCl/SDS buffer, pH 6.8)
SDS-PAGE sample buffer (6X)	30% (v/v) glycerol, 1% SDS, 0.6 M DTT, 0.012% bromophenol blue, 70% (v/v) 4X Tris-HCl/SDS buffer, pH 6.8)
Separating gel (4X Tris-HCl/SDS, pH 8.8)	0.4% SDS, 1.5 M Tris-HCl, pH 8.8
SOC medium	2% bactotryptone, 0.5% bacto-yeast extract, 10 mM NaCl, 2.5 mM KCl, 10 mM MgCl ₂ , 10 mM MgSO ₄ , 20 mM glucose
Stacking gel (4X Tris-HCl/SDS, pH 6.8)	0.4% SDS, 0.5 M Tris-HCl, pH 6.8
TAP Buffer	150 mM NaCl, 10mM Tris, pH 8.0

TAE (50X)	2 M Tris, 5.71% (v/v) glacial acetic acid, 50 mM EDTA, pH 8.0
Transfer buffer	25 mM Tris-HCl, 190 mM glycine, 20% (v/v) methanol, 2.5% (v/v) isopropanol
T-TBS	50 mM NaCl, 0.5% (v/v) Tween-20, 20 mM Tris-HCl, pH 7.5

2.2 Antibodies

Tables 2.2.1 and 2.2.3 below list primary antibodies used for immunofluorescence (IF) and immunoblotting, respectively. Secondary goat antibodies conjugated with either Alexa 488 or Alexa 594 were obtained from Molecular Probes and used at 1:600 dilution for IF. Immunoblots were revealed using either film or a LI-COR apparatus (LI-COR Biosciences) apparatus. For film exposure, horseradish peroxidase (HRP)-conjugated goat anti-rabbit IgG secondary antibodies were purchased from Bio-Rad Laboratories and used at 1:2500 dilution. For the LI-COR procedure, secondary goat antibodies conjugated with either Alexa 690 or Alexa 750 were obtained from Molecular Probes and used at 1:5000.

Table 2.2.1 Primary antibodies used in IF

Primary Antibody	Dilution	Type	Source
Mouse anti- β -coatomer protein	1:300	Monoclonal	Dr. T. Kreis; University of Geneva, Geneva, Switzerland; (Allan and

(clone M3A5)			Kreis, 1986)
Mouse anti-GM130	1:1000	Monoclonal	BD Transduction Laboratories
Mouse anti-Myc (clone 9E10)	1:500	Monoclonal	Invitrogen
Mouse anti-p115 (clone 7D1)	1:50	Monoclonal	Dr. Gerry Waters; Princeton University, US
Rabbit anti-Giantin	1:2000	Polyclonal	Covance
Rat anti-hemagglutinin (HA)	1:50	Monoclonal	Roche Diagnostics

Table 2.2.2 Primary antibodies used in immunoblotting

Primary Antibody	Dilution	Type	Source
Mouse anti-myc (clone 9E10)	1:500	Monoclonal	Invitrogen
Rabbit anti-GFP	1:50000	Polyclonal	Dr. Luc Berthiaume; University of Alberta, Canada

2.3 Cell culture

The cell lines used for the work described in this thesis include Hela cells (ECACC; Sigma-Aldrich, 93021013) and BGMK cells (a gift from Dr. Evans). These lines were maintained at 37°C in a 5% CO₂ incubator in Dulbecco's modified

Eagle's medium (DMEM) supplemented with 10% FBS, 100 µg penicillin/ml medium, and 100 µg streptomycin/ml medium, and 2mM L-glutamine. For live cell imaging experiments, cells were transferred to CO₂ independent DMEM supplemented with 10% FBS.

2.4 Construction of plasmids

2.4.1 Arf dominant negative and constitutively active proteins tagged with Green Fluorescence Protein (GFP) and or the haemagglutinin (HA) epitope.

The plasmids used for production of these Arf mutants were either the pEGFP-N1 (Clontech, Mountain View, CA) or the pcDNA 4/TO(-) HA (Manolea et al., 2010). Fragments encoding Arf1 Q71L, Arf4 Q71L, and Arf4 NI were inserted into pEGFP-N1 and pcDNA 4/TO HA(-) between the Xho1 and Kpn1 sites, whereas the Arf4 T31N was inserted only into pcDNA 4/TO HA(-). Specifically for pEGFP-N1, the first three fragments were obtained by PCR amplification from vectors containing untagged Arf mutant sequences using forward primers containing the Xho1 site upstream of the ATG start codon, and reverse primers that altered the TGA stop codon to CGC by introduction of a Kpn1 restriction site allowing for an in-frame translation of GFP (refer to table 2.4.3 for primer sequences). This approach introduced a linker between Arf and GFP of 12 amino acids (AVPRARDPPVAT). The same three fragments were inserted into the pcDNA 4/TO(-) HA with the same restriction sites. The fragment encoding Arf4 T31N was directly cut from the pEGFP-N1 plasmid and inserted into the pcDNA 4/TO(-). The

untagged mutant templates were created from Dr. Mary Schneider and the Arf4 T31N-GFP template was created by Dr. Justin Chun.

2.4.2 Arf4 G2A tagged with HA and Arf4 T31N G2A tagged with GFP

These plasmids were constructed by inserting a fragment encoding Arf4 G2A into the pcDNA 4/TO(-) HA and inserting the fragment encoding Arf G2A T31N into pEGFP-N1. These fragments were derived by PCR amplification on Arf4 or Arf4 T31N vectors containing either Arf4 wt or Arf4 T31N. Forward primers introduced an Xho1 restriction site upstream of the ATG start codon and a G2A mutation, whereas the reverse primers introduced a Kpn1 restriction site where the original stop codon was resulting in in-frame translation of GFP linked by a 12 amino acid chain (AVPRARDPPVAT). The linker in the pcDNA 4/TO(-) HA that arose from the Kpn1 site, matched the first three amino acids of the pEGFP-N1 linker (AVP).

2.4.3 Arf4 T31N chimeras tagged with GFP

These chimera mutants were constructed by either PCR amplification or site directed mutagenesis using the QuickChange kit (Stratagene, La Jolla, CA). The mutants obtained by PCR amplification incorporated the Xho1 restriction site upstream of the ATG start codon in the forward primer and introduced the Kpn1 restriction site to the location of the original stop codon in the reverse primer. This allowed for the in-frame translation of GFP linked by the 12 amino acid chain (AVPRARDPPVAT). The Arf4 T31N template used to obtain these fragments

was constructed by Dr. Justin Chun. Several mutants were constructed using repeated site directed mutagenesis performed as per QuickChange Kit manufacturer's instructions (Stratagene, La Jolla, CA).

Table 2.4.1 Summary of Arf4 T31N chimera's obtained

Introduced mutation in Arf4 T31N	Alternate name	Method	Template(T31N background)
L3N T4I S10K R11G Q17E	$\alpha 0$	PCR	Arf4-GFP
T164D E176Q S178R R180Q	$\alpha 6$	PCR	Arf4-GFP
A104R Q108M	$\alpha 3$	Site directed mutagenesis	Arf4-GFP
S137A	$\alpha 4$	Site directed mutagenesis	Arf4-GFP
Q146H T152N	$\beta 6$	Site directed mutagenesis	Arf4-GFP
L3N T4I S10K R11G Q17E C62S	$\alpha 0\beta 3$	PCR	Arf4 $\alpha 0$ -GFP
A104R Q108M S137A	$\alpha 3\alpha 4$	Site directed mutagenesis	Arf4 $\alpha 3$ -GFP
S137A Q146H T152N	$\alpha 4\beta 6$	Site directed mutagenesis	Arf4 $\alpha 4$ -GFP
Q146H T152N T164D E176Q S178R R180Q	$\beta 6\alpha 6$	PCR	Arf4 $\beta 6$ -GFP
A104R Q108M S137A	$\alpha 3\alpha 4\beta 6$	Site directed	Arf4 $\alpha 4\beta 6$ -GFP

Q146H T152N		mutagenesis	
A104R Q108M S137A	$\alpha 3\alpha 4\beta 6\alpha 6$	PCR	Arf4 $\alpha 3\alpha 4\beta 6$ -
Q146H T152N T164D			GFP
E176Q S178R R180Q			

2.4.4 Arf T31N bridge mutants

The plasmids listed below were all constructed by site directed mutagenesis using the QuickChange kit manufacturer's instructions (Stratagene, La Jolla, CA). The template used was a pEGFP-N1 plasmid with either the Arf4 T31N sequence or Arf1 T31N constructed by Dr. Justin Chun and Dr. Mary Schneider, respectively.

Table 2.4.2 Arf bridge mutants constructed

Mutation introduced into Arf T31N

Arf4 K79R *

Arf4 V113R

Arf 4 K79E V113R

Arf4 K79R V113R*

Arf1 R79K

Arf1 R79E

Arf1 R79A*

Arf1 E113R

Arf1 E113A*

Arf1 R79K E113V

Arf1 R79K E113D

Arf1 R79E E113R

*Constructed by Heber Castillo

Table 2.4.3 Primers used for molecular cloning

Primer name	Sequence	Construct name
Arf1 for	CCA CTC GAG ACC ATG GGG AAC ATC TTC GCC AAC	Arf1 Q71I-HA, Arf1 Q71I- GFP, Arf1 N1-GFP
Arf1 rev	CAC AGG TAC CGC CTT CTG GTT CCG GAG CTG ATT G	Arf1 Q71I-HA, Arf1 Q71I- GFP, Arf1 N1-GFP
Arf4 for	CCA CTC GAG ACC ATG GGC CTC ACT ATC TCC TCC	Arf4 Q71L-HA, Arf4 Q71L- GFP
Arf4 rev	CAC AGG TAC CGC ACG TTT TGA AAG CTC ATT TGA CAG	Arf4 Q71L-HA, Arf4 Q71L- GFP, Arf4 G2A-HA, Arf4 G2A T31N-GFP
Arf4 G2A for	CCA CTC GAG ACC ATG GCC CTC ACT ATC TCC TCC	Arf4 G2A-HA and Arf 4 G2A T31N-GFP
Arf4/1 N for	CCA CTC GAG ACC ATG GGC AAC ATT ATC TCC TCC CTC TTC AAG GGA CTA TTT GGC AAG AAG GAG ATG CGC ATT TTG ATG GTT GGA TTG	Arf4 α 0 T31N-GFP
Arf4/1 C rev	CAC AGG TAC CGC CTG TTT	Arf4 α 6 T31N-GFP

	TCT AAG CTG ATT TGA CAG CCA GTC AAG TCC TTC ATA CAG ACC ATC TCC TTG TGT TGC ACA AGT G	
Arf4 α 3 for	GAA TTC AGG AAG TAA GAG ATG AGC TGA TGA AAA TGC TTC TGG	Arf4 α 3 T31N-GFP
Arf4 α 3 rev	CCA GAA GCA TTT TCA TCA GCT CAT CTC TTA CTT CCT GAA TTC	Arf4 α 3 T31N-GFP
Arf4 β 6 for	CTA GGG CTT CAC TCT CTT CGT AAC AGA AAC TGG TAT GTT C	Arf4 β 6 T31N-GFP
Arf4 β 6 rev	GAA CAT ACC AGT TTC TGT TAC GAA GAG AGT GAA GCC CTA G	Arf4 β 6 T31N-GFP
Arf4 α 4 for	CAA ATG CTA TGG CCA TCG CTG AAA TGA CAG ATA AAC	Arf4 α 4 T31N-GFP
Arf4 α 4 rev	GTT TAT CTG TCA TTT CAG CGA TGG CCA TAG CAT TTG	Arf4 α 4 T31N-GFP
Arf4 β 3 for	GAA TAT AAG AAC ATT TCT TTC ACA GTA TGG G	Arf4 α 0 β 3 T31N-GFP
Arf4 β 3 rev	CCC ATA CTG TGA AAG AAA TGT TCT TAT ATT C	Arf4 α 0 β 3 T31N-GFP
Arf4 V113E for	GCA GAA AAT GCT TCT GGA AGA TGA ATT GAG	Arf4 T31N V113E-GFP

Arf4 V113E rev	CTC AAT TCA TCT TCC AGA AGC ATT TTC TGC	Arf4 T31N V113E-GFP
Arf4 K79R for	GAT AGA ATT AGG CCT CTC TGG AGG CAT TAC TTC CAG AAT AC	Arf4 T31N K79R-GFP
Arf4 K79R rev	GTA TTC TGG AAG TAA TGC CTC CAG AGA GGC CTA ATT CTA TC	Arf4 T31N K79R-GFP
Arf1 E113V for	CTC ATG AGG ATG CTG GCC GTG GAC GAG CTC CGG GAT GC	Arf1 T31N E113V-GFP
Arf 1 E113V rev	GCA TCC CGG AGC TCG TCC TCG GCC AGC ATC CTC ATG AG	Arf1 T31N E113V-GFP
Arf1 R79K for	CCG GCC CCT GTG GAA GCA CTA CTT CCA GAA CAC AC	Arf1 T31N R79K-GFP
Arf1 R79K rev	GTG TGT TCT GGA AGT AGT GCT TCC ACA GGG GCC GG	Arf1 T31N R79K-GFP
Arf1 E113D for	CTC ATG AGG ATG CTG GCC GAC GAC GAG CTC CGG GAT GC	Arf1T31N E113D-GFP
Arf1 E113D rev	GCA TCC CGG AGC TCG TCG TCG GCC AGC ATC CTC ATG AG	Arf1T31N E113D-GFP
Arf1 R79E for	CCG GCC CCT GTG GGA GCA CTA CTT CCA GAA CAC AC	Arf1 T31N R79E-GFP
Arf1 R79E rev	GTG TGT TCT GGA AGT AGT	Arf1 T31N R79E-GFP

	GCT CCC ACA GGG GCC GG	
Arf1 E113R for	CTC ATG AGG ATG CTG GCC AGG GAC GAG CTC CGG GAT GC	Arf1 T31N E113R-GFP
Arf1 E113R rev	GCA TCC CGG AGC TCG TCC CTG GCC AGC ATC CTC ATG AG	Arf1 T31N E113R-GFP
Arf4 K79E for	GAT AGA ATT AGG CCT CTC TGG GAG CAT TAC TTC CAG AAT AC	Arf4 T31N K79E-GFP
Arf4 K79E rev	GTA TTC TGG AAG TAA TGC TCC CAG AGA GGC CTA ATT CTA TC	Arf4 T31N K79E-GFP
Arf4 V113R for	GCA GAA AAT GCT TCT GCG AGA TGA ATT GAG	Arf4 T31N V113R-GFP
Arf4 V113R rev	CTC AAT TCA TCT CGC AGA AGC ATT TTC TGC	Arf4 T31N V113R-GFP
Arf1 R79A for	CCG GCC CCT GTG GGC CCA CTA CTT CCA GAA CAC AC	Arf1 T31N R79A-GFP
Arf1 R79A rev	GTG TGT TCT GGA AGT AGT GGG CCC ACA GGG GCC GG	Arf1 T31N R79A-GFP
Arf1 E113A for	CTC ATG AGG ATG CTG GCC GCG GAC GAG CTC CGG GAT GC	Arf1 T31N E113A-GFP
Arf1 E113A rev	GCA TCC CGG AGC TCG TCC GCG GCC AGC ATC CTC ATG AG	Arf1 T31N E113A-GFP

2.5 Plating and transient transfection of cells

Cells were plated onto glass coverslips that were ethanol sterilized and transferred to 6 well plates. Cells were grown to 40-50% confluency, then transfected with plasmid using TransIT-LTI transfection reagent (Mirus, Madison, WI), as per manufacturer's instructions. Cells were typically examined 12-18 hours post-transfection.

2.6 siRNA knock down

Pool and individual siRNA duplexes were purchased from Dharmacon that targeted human Arf1 (LQ 011580), Arf4 (LQ 011582) or membrin (LU-010980-00-0005). Protocol was done according to the instructions provided by the manufacturer of the oligofectamine (invitrogen) transfection reagent.

Experiments performed during the course of this thesis required the testing of siRNAs as pools and individual pairs to identify conditions for the efficient knock down. This analysis identified as most effective sequences 5 and 6 targeting Arf4 and sequences 6 and 7 targeting membrin. Those were pooled for experiments described in the thesis. A pool of four siRNAs targeting Arf1 was also used. Knock downs were performed for 3 to 4 days with 100 nM of siRNA duplex. Negative controls were done in conjunction by using a siRNA duplex sequence targeting luciferase at 100 nM concentration.

2.7 Immuno-fluorescence

Cells plated on sterilized coverslips were subject to immuno-fluorescence. Cells were washed twice with PBS before fixation for 15 minutes with 3% paraformaldehyde (supplemented with 100 μ M MgCl₂ and 100 μ M CaCl₂). Fixation was stopped with quench buffer (50mM NH₄Cl in PBS) for 10 minutes, followed by incubation with permeabilization buffer (0.1% Triton X-100) supplemented with 0.05% SDS for experiments involving antibody m3A5. Blocking with PBS containing 0.2% gelatin for five minute incubations was performed three times after permeabilization. Cells were then incubated with primary and secondary antibodies, as indicated.

2.8 Fluorescence microscopy

2.8.1 Epifluorescence microscopy

An Axioscop II microscope (Carl Zeiss, Thornwood, NY) with an 63X objective (plan-Apocromat, NA=1.4) was used to acquire images. Digital images were captured with a CoolSNAP HQ (Photometrics) monochrome CCD (Charge-Coupled Device) camera. The images were obtained and exported as 12 bit TIFF files.

2.8.2 Live cell imaging microscopy

Cells grown on round 25 mm coverslips were transferred individually from a 6 well dish to an atto chamber CO₂ independent media supplemented with 10% FBS. A Zeiss Axiovert 200M confocal microscope equipped with an UltraVIEW ERS 3E spinning disk (Perkin Elmer) and 63X objective lens (plan-Apocromat,

NA=1.4) was used to perform live cell imaging. A heated stage was used to maintain cell at 37°C. Images were acquired by a 9100-50 electron multiplier CCD digital camera and processed by Volocity. For BFA addition experiments, 500 µl CO₂ independent media containing 4X BFA was added to the atto chamber containing 1.5 ml of media.

2.9 Cell lysis, fractionation and preparation of cell extracts

siRNA knock down experiments involved analysis of whole cell lysates, whereas Arf4 T31N localization studies required sub-cellular fractionations prior to SDS PAGE. Cells grown either in wells of a six-well dish or individual 10 cm tissue culture dishes were gathered with either lysis buffer or homogenization buffer after several washes with PBS. After 5 minutes of incubation with lysis or homogenization buffer, a cell scraper was used to gather cells. Cells destined to be homogenized were passed through an 18 micron clearance ball bearing homogenizer 30x on ice. Cell lysates and homogenates were cleared by centrifugation at 8000xg at 4°C. A 6x loading sample buffer was added to the cleared supernatants of cell lysates then heated to 100°C for 10 minutes. Cleared supernatants of cell homogenates were further separated by centrifugation into high speed pellets (microsomal fraction) and high speed supernatants (cytosolic fraction) using the TLA 120.2 rotor (Beckman) at 75,000 RPM at 4°C for 30 minutes. 6x sample buffer was added to both the high speed supernatant and high speed pellet resuspended in homogenization buffer and boiled for 10 minutes.

2.10 SDS-Polyacrylamide gel electrophoresis (SDS-PAGE)

Protein samples were analyzed by SDS-PAGE using Tris-glycine sodium dodecyl sulphate- polyacrylamide gels calibrated with DNA ladders (Bio-Rad Laboratories or Fermentas). Frozen protein samples were thawed and loaded onto 10-15% slab SDS gels at 25 μ l per well. Samples were separated on a 6.5 inch wide slab gel apparatus (CBS Scientific, Del Mar, CA) first through the stacking gel at 80V followed by 120V through the resolving gel.

2.11 Immunoblotting

Once protein samples had been separated by SDS-PAGE, protein samples were analyzed by immunoblotting. Resolved proteins were transferred from the resolving gel to nitrocellulose membranes at 26V overnight in transfer buffer. Two methods were used to immunoblot based upon which system of visualization was used, namely, film or LI-COR. Processing of the immunoblots for the LI-COR system followed manufacturer's instructions (LI-COR Biosciences, Lincoln, NB). Membranes ultimately processed using film underwent Ponceau S (0.1% (w/v) in 5% acetic acid) staining to confirm protein transfer and identify molecular weight markers. Following two rinses with Milli Q ddH₂O, membranes were blocked in TTBS (50mM NaCl, 0.5% (v/v) Tween, 20mM Tris-HCL, pH 7.5) supplemented with 2% milk for one hour on a rocking platform. Membranes were then incubated for one hour in primary antibody diluted in TTBS supplemented with 2% milk. Following primary antibody incubation, the

membranes were washed three times for 10 minute in TTBS. Membranes were then incubated with HRP-conjugated secondary antibodies diluted in TTBS. Detection of HRP-conjugated secondary antibodies required ECL-plus system (GE Healthcare) as per manufacturer's instructions. In a dark room, membranes were exposed to Super RX medical X-Ray film (Fujifilm) in a FBXC 810 autoradiography cassette (Fisher Scientific) for varying lengths of time based upon protein expression levels and developed using the X-OMAT 2000A processor (Kodak).

2.12 Quantitation of Arf release kinetics

Imaris software was used to quantitate the release of Arf from the Golgi over a period of 5 minutes. Three experimental situations were quantitated; Arf1-GFP, Arf1 T31N R79E-GFP, or Arf1 T31N-GFP co-expressed with myc-membrin. Videos acquired on the Axiovert 200M confocal microscope were exported as OME files and analyzed on Imaris. Regions corresponding to the Golgi complex were masked in 3D based on intensity and the mask was duplicated through all timepoints. An outline of the whole cell was carefully drawn by hand and extended throughout the z stacks and in all timepoints. To measure background, a small circle was drawn in a region away from cells and approximately the size of a nucleus was; this circle was then extended throughout the z stacks and time points. The intensity mean and surface area were obtained for the objects created. The following equation was used to solve for the intensity at the Golgi complex:

$$\text{Golgi signal} = \frac{\text{Golgi}_A (\text{Golgi}_{\text{Int}} - \text{Cell}_{\text{Int}})}{\text{Cell}_A (\text{Cell}_{\text{Int}} - \text{Background}_{\text{Int}})} \quad \text{A=Surface Area, Int=Intensity}$$

mean

At least 4 cells were used per experimental situation over at least three separate experiments. The BGMK studies used the same quantitation described above.

CHAPTER THREE: RESULTS

3.1 “GDP-arrested” mutant forms of Arf4 associate with peripheral puncta

Justin Chun previously demonstrated that Arf4•GDP associated with ERGIC but not the Golgi complex by using two different drugs and by using the “GDP arrested” mutant Arf4 T31N. In contrast, work subsequently published by van Kuppeveld and colleagues proposed that Class II Arf activation was BFA insensitive at both the ERGIC and Golgi complex in BGMK cells (Daniel *et al.*, 2008). I wanted to confirm that the unique localization Arf4•GDP at ERGIC reported by Dr Chun was real and not the result of aggregation or interference by the GFP tag. Our approach was to use an Arf4 T31N mutant tagged with the smaller HA epitope, analyze a different “GDP-arrested” Arf4 mutant, and finally repeat Arf4 observations in BGMK cells.

I first examined whether the “GDP-arrested” Arf4 T31N-HA and the “fast cycling” Arf4 N126I-GFP mutants were also preferentially localized to peripheral puncta. It has been documented that GFP, a large reporter protein can interfere with the function of your protein of interest and yield misleading results (Kahn *et al.*, 2010). As previously observed with Arf4 T31N-GFP by Dr. Justin Chun, Arf4 T31N-HA also associated with peripheral puncta (Figure 3.1). Similarly, Arf4 N126I-GFP also localized primarily at puncta, although the relative number and size of puncta appeared lower in comparison with those

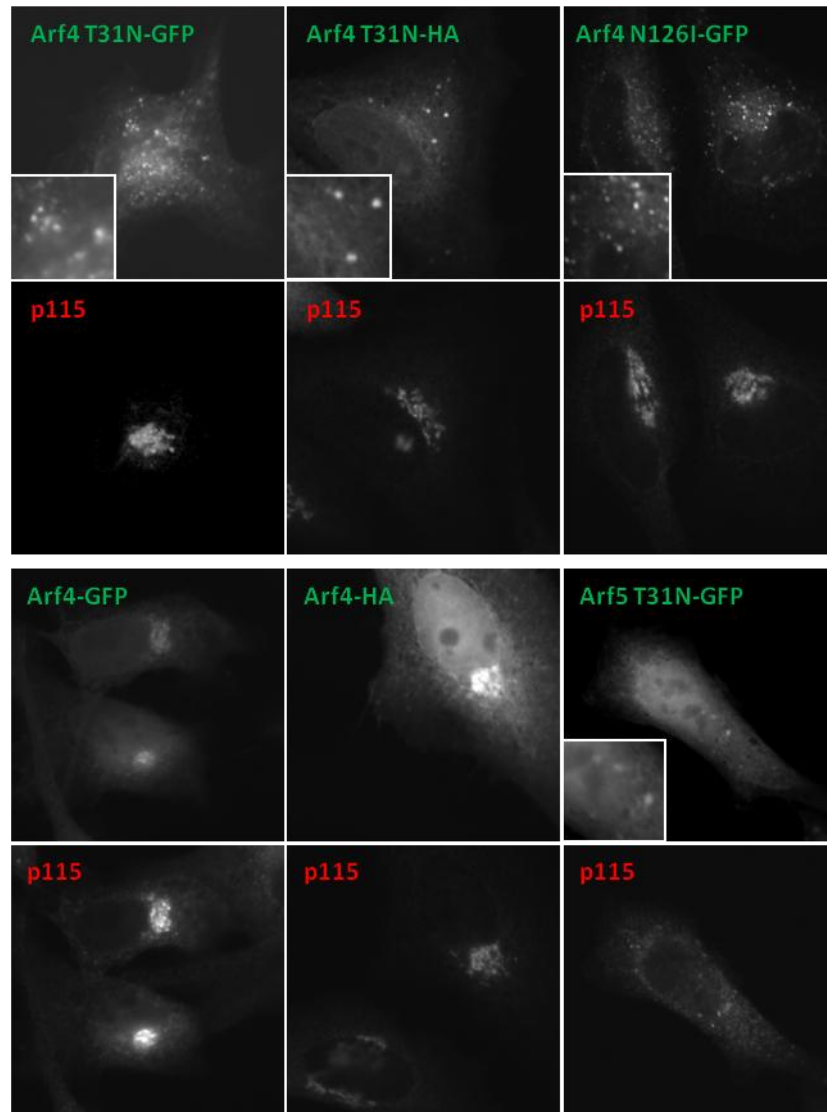


Figure 3.1. GDP-arrested mutants of Arf4 associate with peripheral puncta irrespective of the nature of tag or mutation.

HeLa cells were transfected with plasmids encoding Arf4-GFP, Arf4 T31N-GFP, Arf4 N126I-GFP, Arf4-HA, Arf4 T31N-HA, or Arf5 T31N-GFP. Cells were fixed after 18 hours and labelled with anti-p115 and or anti-HA antibodies. These images were acquired with an epifluorescence microscope and are representative of at least three separate experiments. Bars, 20 μ m. Insets show 2x magnification of region of interest.

observed with Arf4 T31N-GFP (Figure 3.1). Interestingly, in addition to the peripheral puncta localization, Arf4 T31N frequently displayed a weak reticular pattern reminiscent of the ER. We chose to focus on only the association of Arf4 with ERGIC, as the wt form of Arf4 associates primarily with the Golgi and ERGIC and not the ER.

A significant portion of this thesis was based upon the observation that inactive Arf4•GDP was recruited to ERGIC and not the Golgi complex. However, as mentioned above, it was reported in BGМК cells that unlike Arf1, Arf4 would remain Golgi-bound after treatment with BFA for five minutes (Duijsings *et al.*, 2008). This could have occurred if Arf4 activation was BFA resistant or if an Arf4•GDP receptor was present at the Golgi complex in these cells. To examine these possibilities we obtained the BGМК cell line from Dr. D. Evans and repeated their experiments. We found that upon BFA treatment Arf1-GFP was quickly released from Golgi membranes, as expected (Figure 3.2). To our relief, Arf4-GFP was similarly released from Golgi membranes after a couple of minutes of BFA treatment (Figure 3.2). These results confirm that Arf4 activation at the Golgi is BFA sensitive and that Arf4•GDP does not remain associated with the Golgi. Overall, my data suggest that localization of Arf4•GDP to puncta does not result from aggregation or tags because changing the tag or mutation does not affect distribution. The localization pattern seems to apply to BGМК cells as well as Arf4-GFP is released from the Golgi complex after the addition of BFA. We have no explanation for the discrepancy with the Duijsings *et al.*, study.

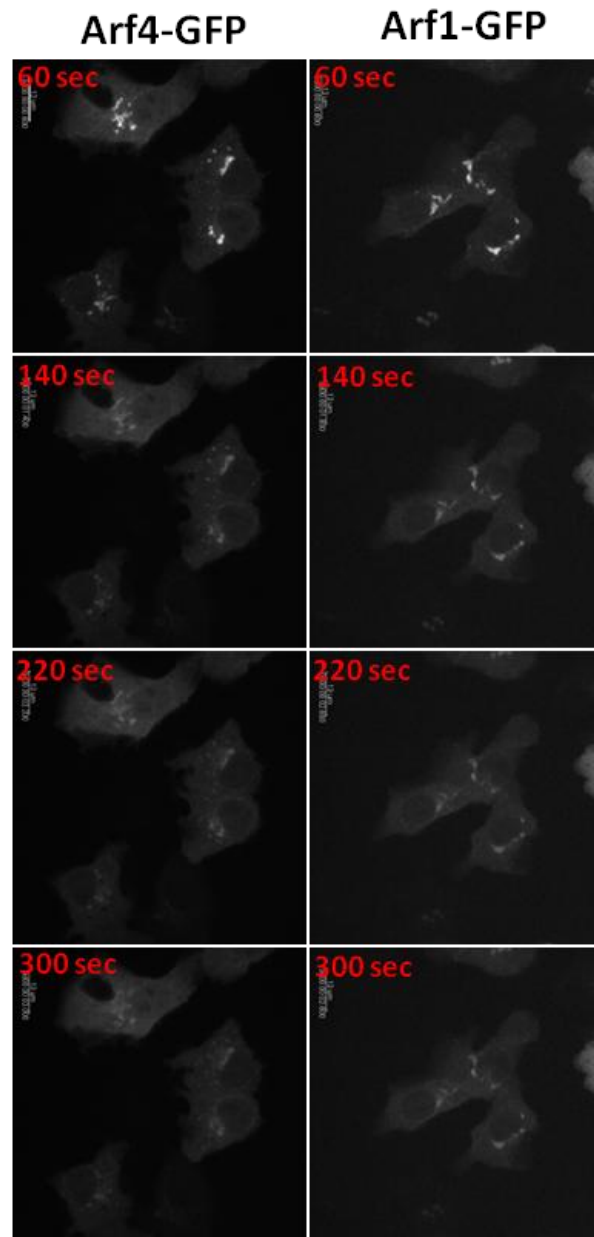


Figure 3.2. BFA treatment causes dissociation of both Arf1 and Arf4 even in BGMK cells.

BGMK cells were transfected with plasmids encoding Arf1-GFP or Arf4-GFP. Live cells were imaged after 18 hours using a spinning disk confocal microscope. Snapshots of single timepoints were acquired at time of BFA addition (60 seconds) and every 80 seconds there after. Images are representative of three separate experiments.

3.2 Arf4 siRNA knock down has no impact on Golgi complex integrity

Studies have shown that single Arf knock down using shRNA had no impact on the secretory pathway (Volpicelli-Daley *et al.*, 2005). We wanted to investigate whether or not Arf4 performed an independent and required function in the secretory pathway by using a more effective knock down approach based on siRNA duplexes. To confirm the efficacy of the Dharmacon duplexes, I measured potential knock down using exogenously expressed tagged protein since no Arf4 antibodies were commercially available. HeLa cells were co-transfected with plasmid encoding Arf4-GFP and either single siRNA duplexes or a pool of all four duplexes for 24 hours to test their relative effectiveness. Analysis by immunofluorescence established that co-transfection of some of the Arf4-targeted siRNAs caused a dramatic reduction in the number Arf4-GFP-expressing cells (Figure 3.3A). Of the four duplexes used, duplex 6 and 8 were the most effective. After this, we conducted biochemical assays to confirm these results. As seen in Figure 3.3B, western blots did indeed confirm that Arf4-GFP levels were dramatically reduced and that the siRNA duplexes 6 and 8 were most effective. Interestingly, the Arf4-GFP does not migrate as a single band but rather as a doublet. This could result from variations in post-translational modification such as myristoylation or mono-glutathionation (Berger *et al.*, 1998).

Now with these results confirmed, we wanted to look at how treatment with duplexes 6 and 8 to reduce endogenous Arf4 would impact the secretory pathway. I treated HeLa cells for 24 hours, 48 hours, and 72 hours and then

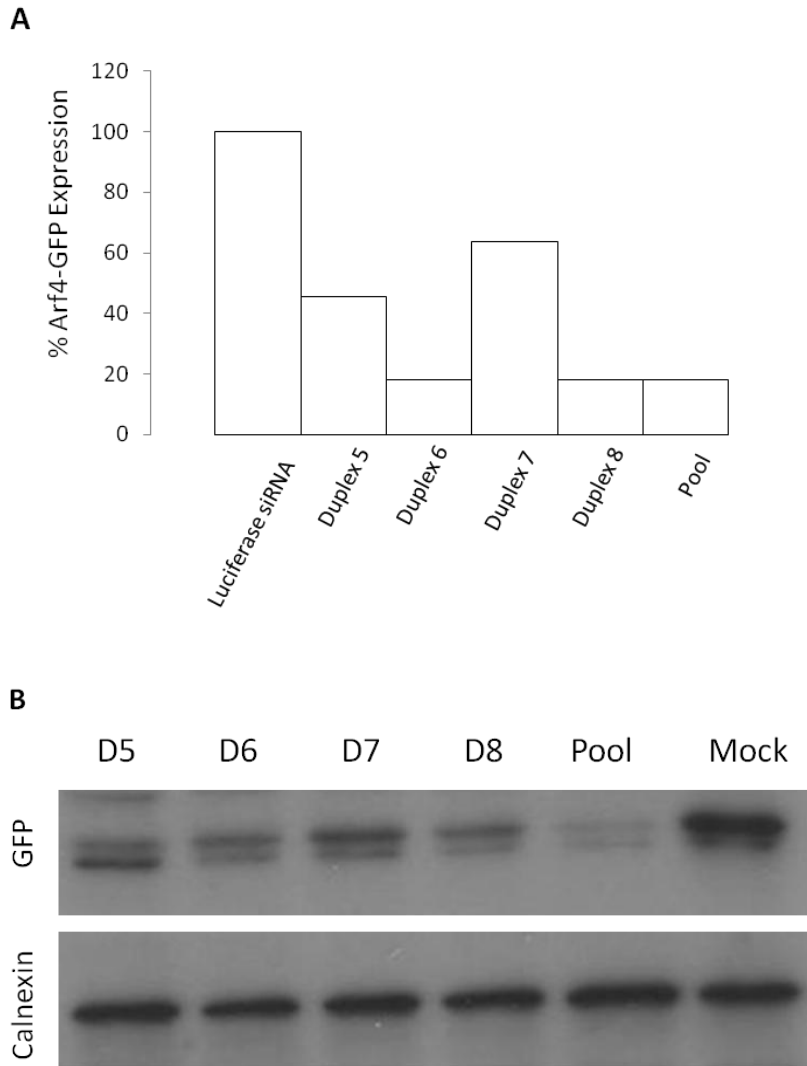


Figure 3.3. Treatment with siRNAs effectively reduces exogenous Arf4-GFP expression.

A. Quantitation of Arf4-GFP siRNA knock down efficacy. HeLa cells were co-transfected with plasmid encoding Arf4-GFP and the indicated siRNA's. After 18 hours, cells were fixed, stained for DAPI and images were obtained using an epifluorescence microscope. The percentage of GFP-positive cells was determined by examining >200 cells per coverslip. **B.** HeLa cells were co-transfected with plasmid encoding Arf4-GFP and the indicated siRNA duplex for 18 hours as described in Chapter 2. Cells were lysed and equal protein amounts were analyzed by SDS-PAGE and immunoblotting using GFP and calnexin antibodies. The blot shown is representative of two separate experiments.

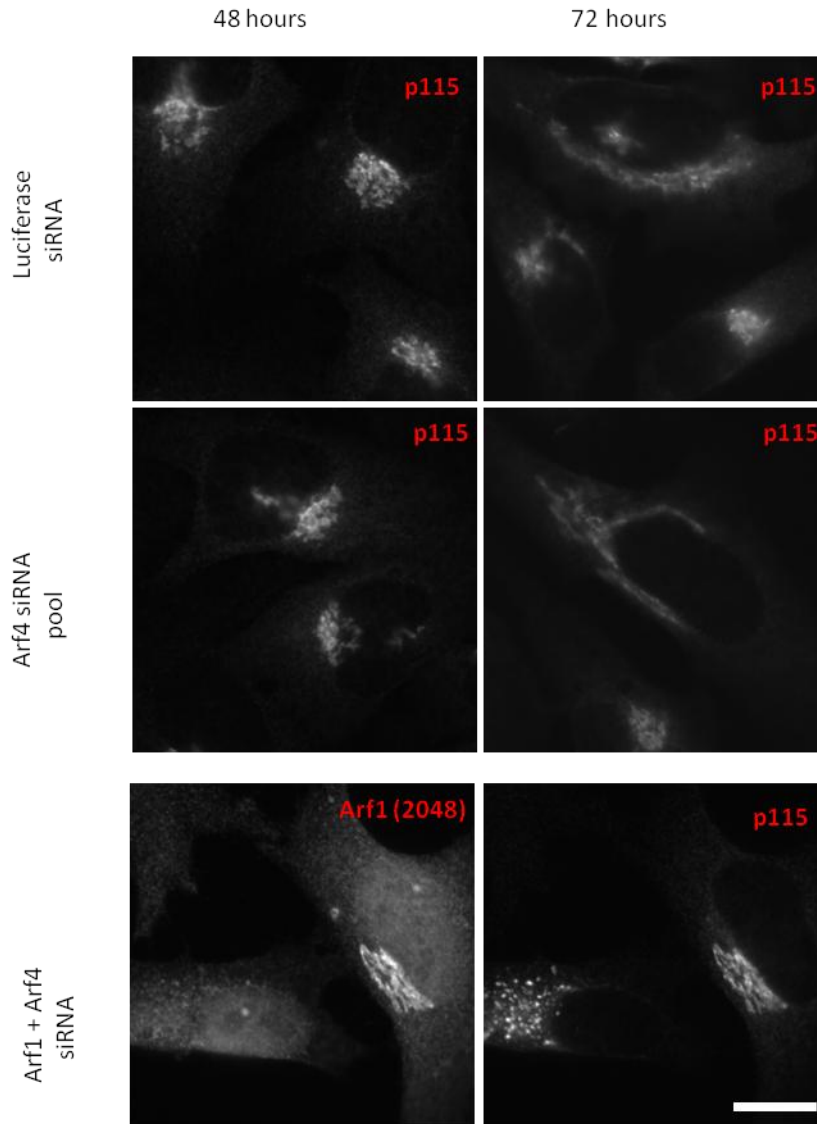


Figure 3.4. The Golgi complex remains intact after treatment with Arf4-targeted siRNAs

Hela cells were transfected with the indicated siRNAs for 48 to 72 hours. Cells were fixed and labelled for p115. Images were acquired using an epifluorescence microscope and are representative of two independent experiments. Double knock down with both Arf1 and Arf4 siRNAs shown at bottom was performed as positive control once for 48 hours. Bar, 20 μ m.

examined transfectants for visible changes in the distribution of p115, a well characterized marker of the Golgi. As can be seen in Figure 3.4, the Golgi remained intact and displayed a normal morphology, even after 72 hour treatment. Unfortunately, we do not have an antibody that detects endogenous Arf4, and so we cannot be sure levels were truly reduced. To provide a positive control of Arf4 knock down, I reproduced a result published by Kahn's group (2005) that showed a double knock down of Arf1 and Arf4 dispersed the Golgi (Figure 3.4). There was no visible impact on the Golgi after 72 hours of single Arf4 knock down, whereas in 48 hours of Arf1 and 4 double knock down, a clear disruption of the Golgi could be seen, suggestive that Arf4 single knock down does not disperse the Golgi. A single knock down of Arf1 was not performed; therefore, it is possible that the fragmented Golgi was a result of just Arf1 knock down and not the combination of Arf1 and Arf4. This is unlikely, as others have shown single Arf1 knock down had no impact on the Golgi complex (Volpicelli-Daley et al., 2005; Boulay et al., 2008). Although my data suggest Arf4 knock down had no impact on the Golgi, there is the possibility that the knock down was not effective enough and that more effective knock down may be needed to observe a phenotype. Alternatively, more sensitive assays of ERGIC function may be required to observe effects of Arf4 knock down. Such assays are discussed in Chapter 4.

3.3 Myristoylation is required for association of Arf4-GDP mutants with ERGIC membranes.

As was mentioned in the introduction, myristoylation of glycine at the N-terminus of Arfs plays an important part in membrane binding; without myristoylation, Arfs lose their normal function (Haun et al., 1993). To better establish that appearance of Arf4•GDP in peripheral puncta truly represents association with ERGIC, I examined whether abolishing myristoylation of Arf4 would eliminate ERGIC binding. I constructed myristoylation-deficient mutants of Arf4 and Arf4 T31N by swapping glycine at position 2 for alanine. Analysis of transfectants co-expressing either Arf4 and Arf4 G2A or Arf4 T31N and Arf4 G2A T31N, revealed that neither of the G2A mutants associated with the Golgi or ERGIC (Figure 3.5). To confirm differences in membrane binding of wild type, G2A and T31N mutants biochemically, I analyzed subcellular fractions by immunoblots. As shown in Figure 3.6A, a significant amount of Arf4 T31N was recovered in the membrane fractions, whereas little was recovered for both wild type and G2A variants. *In vivo*, Arfs display Golgi association; however, this association appears rapidly reversible since *in vitro* assays such as subcellular fractionation reveal Arfs to remain primarily cytosolic (Yan et al., 1994). Again, the doublet band appears, most likely representing myristoylated vs. non-myristoylated Arf. Figure 3.6B shows a quantitative analysis of the fraction of membrane-bound Arf relative to total Arf (membrane plus cytosol). Arf4 T31N displays a 20 fold increase in membrane binding relative to Arf4 T31N G2A.

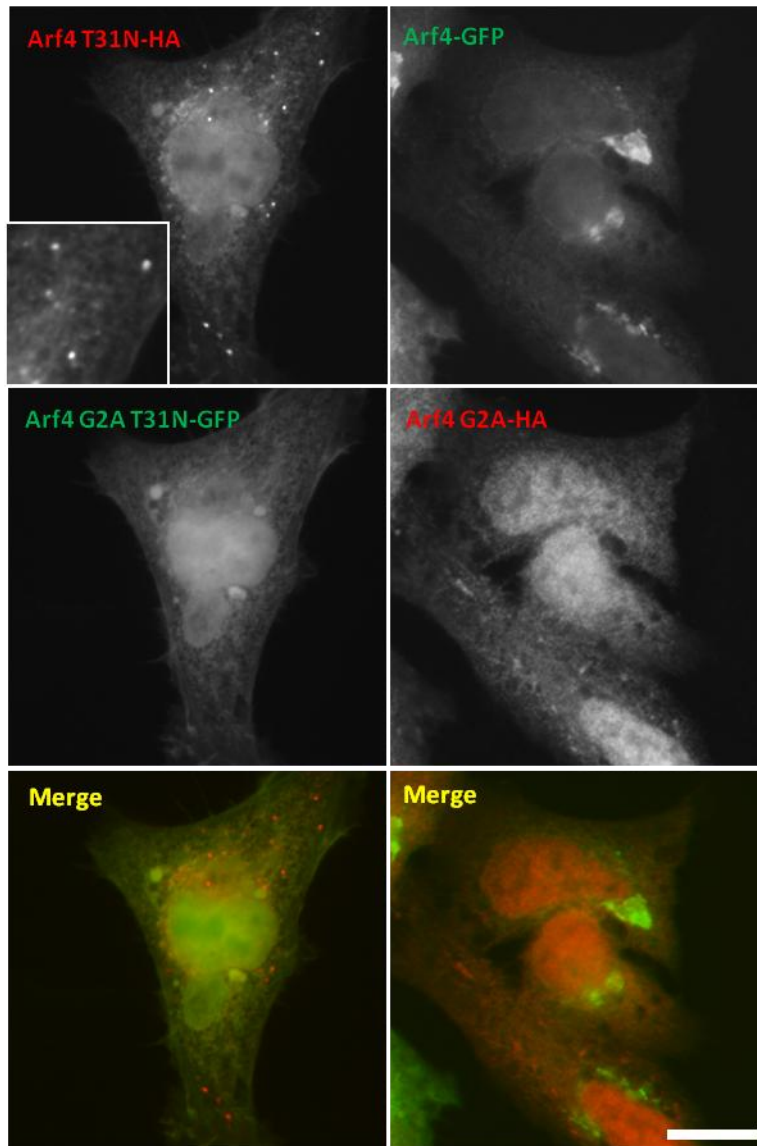


Figure 3.5. Myristoylation at glycine 2 of Arf4 is required for membrane binding

HeLa cells were co-transfected with plasmids encoding either Arf4-GFP and Arf4 G2A-HA or Arf4 T31N-HA and Arf4 G2A T31N-GFP. Cells were fixed after 18 hours and labeled with anti-HA antibodies and images were acquired on an epifluorescence microscope. These images are representative of two separate experiments. Bar, 20 μ m. Inset shows 2X magnification of region of interest.

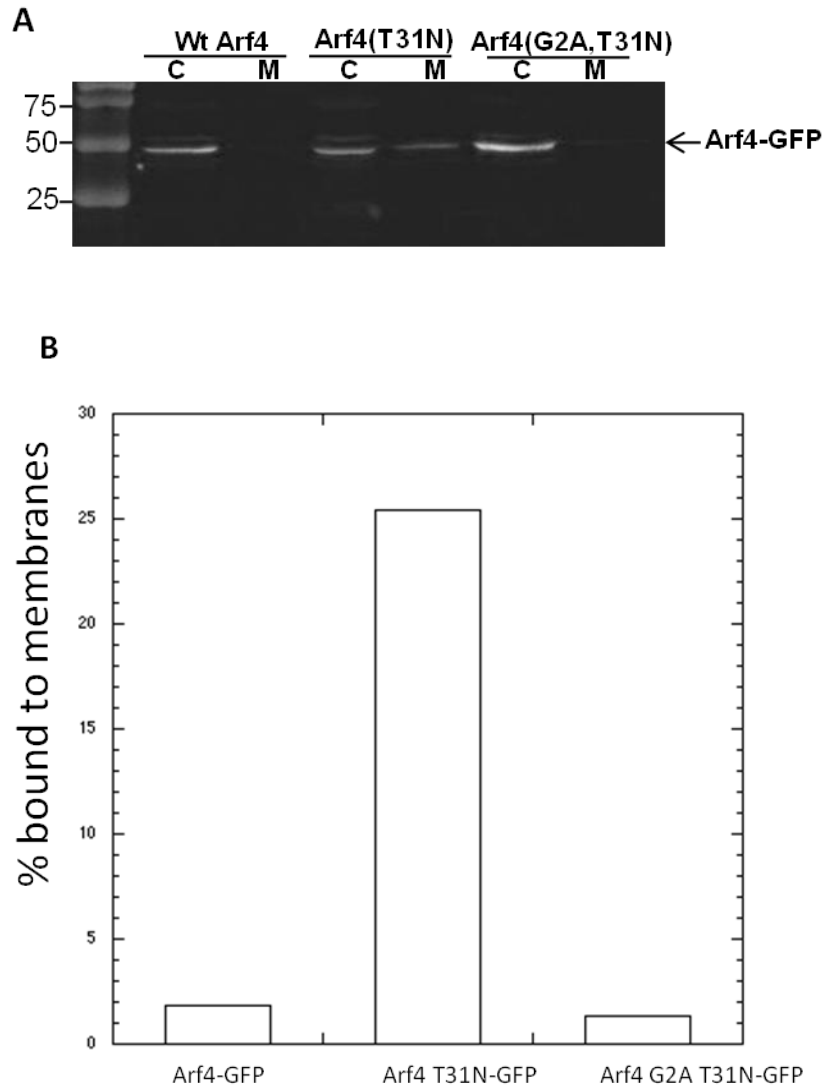


Figure 3.6. Subcellular fractionation confirms importance of myristoylation in membrane binding

A. HeLa cells were transfected with plasmids encoding Arf4-GFP, Arf4 T31N-GFP, or Arf4 G2A T31N-GFP. After 18 hours, cells were homogenized and fractionated into cytosolic and membrane fractions. Equal amounts of protein were analyzed by SDS-PAGE and immunoblotting using anti-GFP antibodies. LI-COR was used to visualize the immunoblots. **B.** Intensity of bands were quantified to confirm degree of membrane binding.

These results confirm that the G2A mutant is unable to bind membrane and that Arf4 T31N binds membranes stronger than the wt. We conclude that Arf4•GDP localization to ERGIC can be abolished by eliminating myristoylation, further supporting that it truly associates with ERGIC and does not result from aggregation. Future experiments to identify an Arf4•GDP receptor by immunoprecipitation assays will take advantage of the Arf4 T31N G2A mutant as a negative control.

3.4 Four early secretory SNAREs unlikely to recruit Arf4-GDP at ERGIC

Our working hypothesis is that the unique recruitment of Arf4 to ERGIC is mediated by a receptor predominantly found at ERGIC. To identify potential Arf4•GDP receptors, we first used a candidate approach. Since previous work established that Arf1•GDP binds the early secretory SNARE membrin (Honda *et al.*, 2005), we hypothesized that Arf4 T31N had a similar type of receptor. A literature search identified membrin along with three other SNAREs, rbet1, syntaxin 5, and sec22b that functioned at the early secretory pathway (Hay *et al.*, 1997; Hay *et al.*, 1996). Since no antibodies were commercially available to these SNAREs, we obtained four plasmids encoding tagged forms of these SNAREs from Dr. Jesse Hays. First, I confirmed the localization of these four SNAREs. I restricted my analysis to transfectants expressing moderate SNARE levels as I had previously found that high over-expression of both HA-syntaxin 5 and myc-membrin caused reproducible fragmentation the Golgi. I confirmed that myc-membrin localizes primarily to *cis*-Golgi structures positive for the Golgi marker

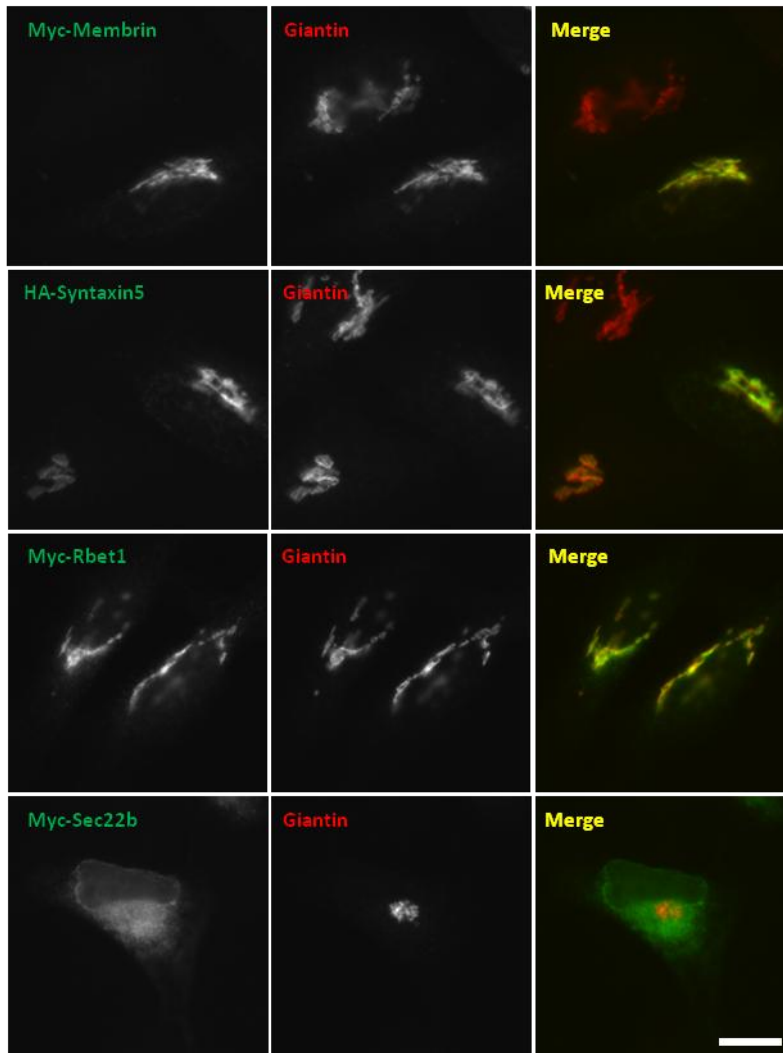


Figure 3.7. Localization of early secretory SNAREs

Hela cells were transfected with plasmids encoding myc-membrin, HA-syntaxin 5, myc-rbet1, or myc-sec22b. After 18 hours, cells were fixed and stained for endogenous giantin, HA, or myc epitopes. Images were acquired by epifluorescence microscopy. These images are representative of at least 2 separate experiments. Bar, 20 μ m.

giantin (Figure 3.7). HA-syntaxin 5 and myc-rbet1 also localized to juxtannuclear structures containing giantin; in contrast, myc-sec22b localized to a reticular pattern reminiscent of the ER (Figure 3.7). Importantly, none of the SNAREs expressed were restricted to peripheral puncta. These results suggest that it is unlikely that any of these SNAREs would be responsible for recruitment of Arf4 T31N to peripheral ERGIC.

The experiments described above do not eliminate the possibility that Arf4•GDP associates selectively with one of the four early SNAREs *in vivo*. Before testing this possibility, I examined the known interaction between membrin and Arf1. Specifically, I compared the relative impact of SNARE over-expression on the localization and dominant negative impact of Arf1 T31N-GFP on the Golgi. As expected, myc-membrin over-expression not only protected the Golgi from disruption by Arf1 T31N-GFP but also caused its accumulation on membrin-positive structures (Figure 3.8). In contrast, over-expression of rbet 1, syntaxin 5, or sec22b did not rescue Arf1 T31N induced Golgi disruption (Figure 3.8). The Golgi SNAREs rbet 1, syntaxin 5 localized instead to peripheral puncta that likely correspond to ERGIC while sec22 remained at the ER where it may colocalize with some Arf1 T31N. These results confirm that Arf1•GDP associates with myc-membrin and suggest that this association is selective since it was the only SNARE tested that prevented Arf1 T31N-induced Golgi disruption.

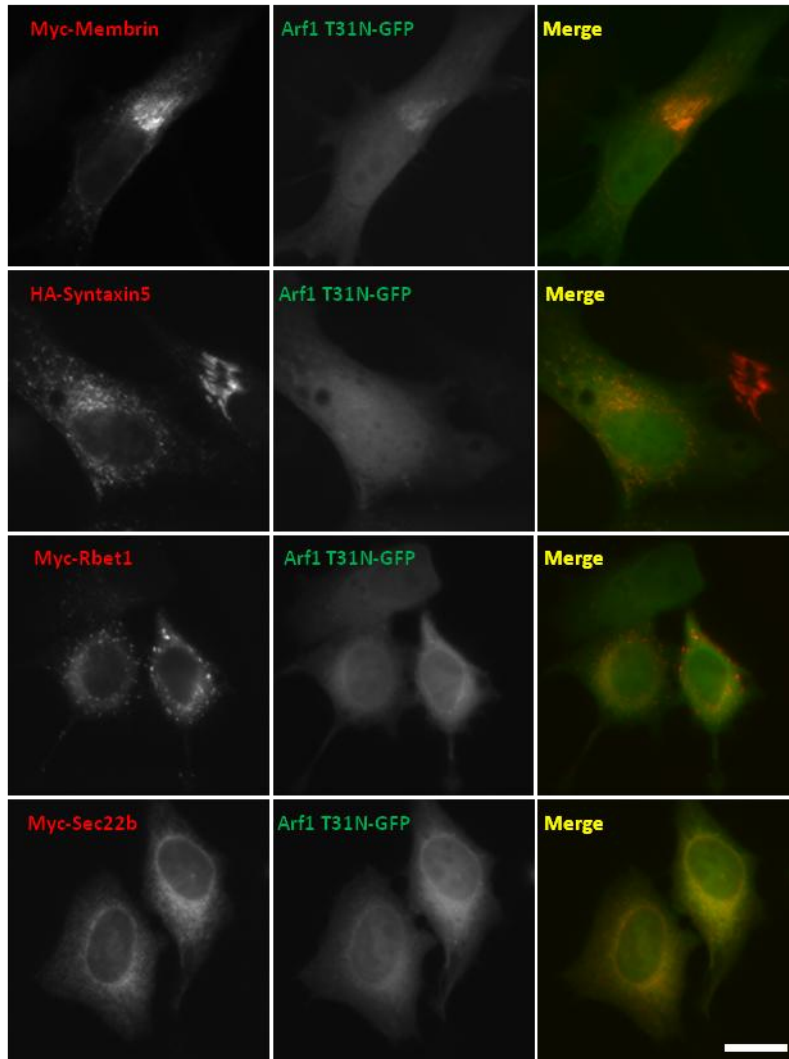


Figure 3.8. Membrin over-expression alters the distribution of Arf1 T31N

HeLa cells were co-transfected with plasmids encoding Arf1 T31N-GFP and either myc-membrin, HA-syntaxin 5, myc-rbet1, or myc-sec22b. After 18 hours, cells were fixed and stained with either anti-HA or anti-myc antibodies. Images were acquired by epifluorescence microscopy. These images are representative of at least 2 separate experiments. Bar, 20 μ m.

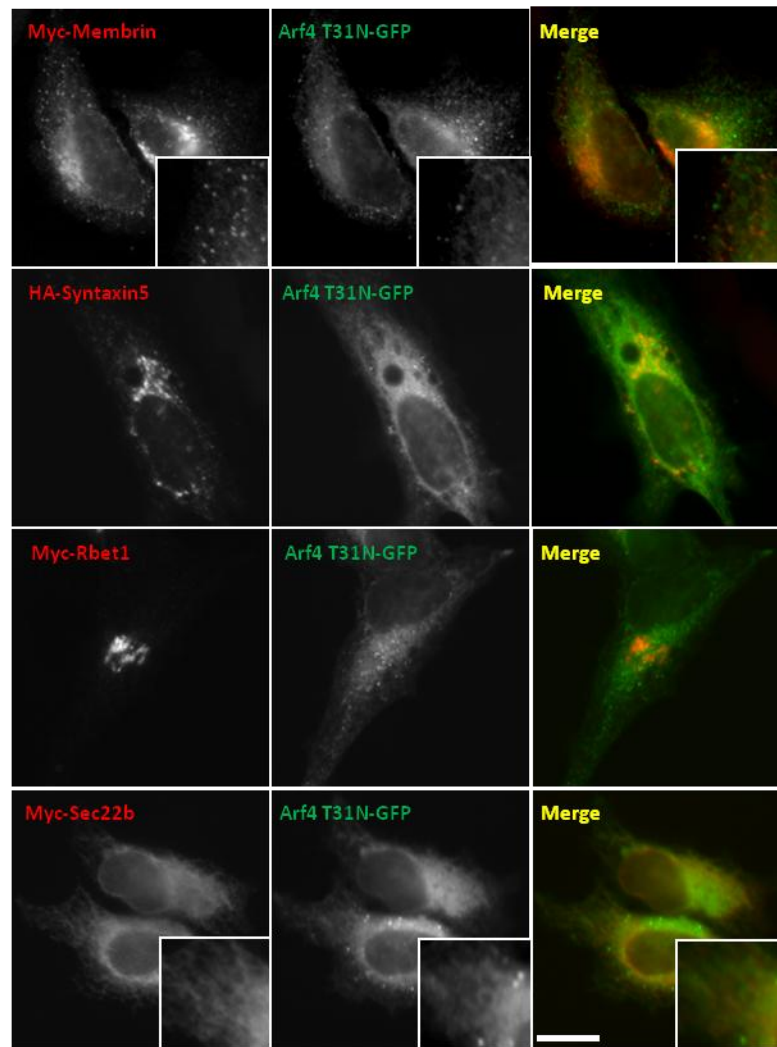


Figure 3.9. None of the early secretory SNAREs alter the localization of Arf4 T31N

Hela cells were co-transfected with plasmids encoding Arf4 T31N-GFP and either myc-membrin, HA-syntaxin 5, myc-rbet1, or myc-sec22b. After 18 hours, cells were fixed and stained with anti-HA or anti-myc antibodies. Images were acquired by epifluorescence microscopy. These images are representative of at least 2 separate experiments. Bar, 20 μ m. Insets show 2x the magnification of region of interest.

To determine if Arf4 can also interact selectively with one of these SNAREs, I co-expressed both Arf4 T31N-GFP and each of the four SNAREs. Over-expression of myc-membrin seemed to promote slight Arf4 T31N Golgi binding (Figure 3.9, top panels). Neither HA-syntaxin 5 nor myc-rbet1 over-expression promoted Arf4 T31N recruitment to the Golgi complex (Figure 3.9). The final SNARE examined, myc-sec22b, still yielded an ER like localization pattern even in the presence of Arf4 T31N-GFP (Figure 3.9). Although no overlap of sec22b was observed with Arf4 T31N at puncta, Arf4 appeared to acquire a reticular pattern that overlapped with that of Sec22b. These results confirm that Arf4•GDP recruitment to peripheral puncta most likely does not involve membrin, sec22b, rbet1, or syntaxin 5, although Arf4•GDP may have a slight affinity for membrin at the Golgi and an affinity for sec22b at the ER. As mentioned in Figure 3.1, some Arf4 T31N may associate with the ER; whether sec22b enhances association of Arf4 with the ER was not investigated. A candidate approach did not yield clear results and therefore I chose to examine instead properties of Arf4 required for ERGIC targeting.

3.5 Identifying residues in Arf4 that may be important to target ERGIC

To further characterize Arf4 membrane binding, I searched for Arf4 residues targeting it specifically to ERGIC. We reasoned that since Arf4 and 5 both bind peripheral puncta in the GDP-bound state whereas Arf1 does not, residues restricted to Arf4 and 5 would represent potential candidates to target to ERGIC.

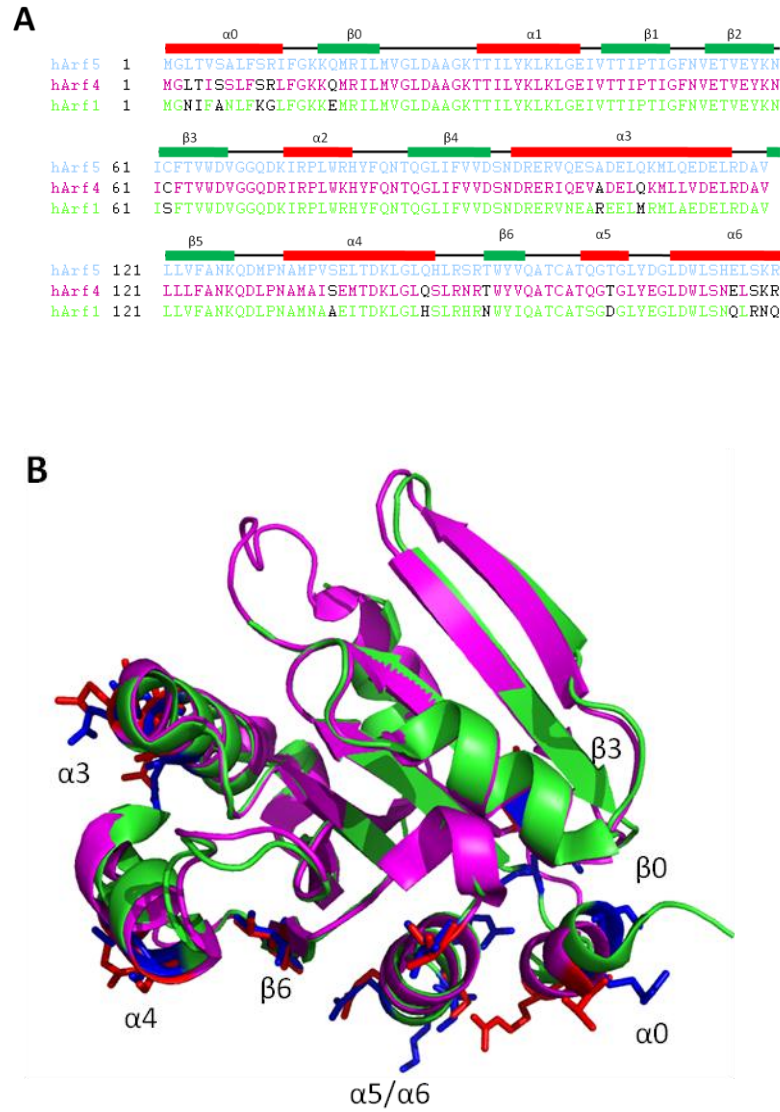


Figure 3.10. Alignment of the sequences of Arf1, 4, and 5 identifies 17 residues conserved in Arf4 and 5 but divergent in Arf1

A. Highlighted residues in black were found to be conserved in Arf4 and 5 but not in Arf1. Red and green rectangles above the alignment indicate alpha helices and β sheets, respectively. **B.** Crystal structures of Arf1 (green) (Amor *et al.*, 1995) and Arf4 (purple) (Choe *et al.*, 2005) were altered in pymol to highlight bolded residues from **A** as red (Arf4) or blue (Arf1) stick diagrams.

I aligned Arf1, 4, and 5 and identified 17 residues conserved in Arf4 and 5 but divergent from Arf1 (Figure 3.10A). Two of the residues were overlooked or determined too similar to mutagenize, leaving 15 residues for testing. To better visualize the relative positions of these residues in the Arf4 structure, we manipulated the crystal structures of Arf1 (Amor *et al.*, 1995) and Arf4 (Choe *et al.*, 2005) using the program pymol (Figure 3.10B). To test the involvement of these residues we chose to progressively transform Arf4 T31N into Arf1 T31N by site directed mutagenesis.

Before mutagenesis, we first had to establish that by mutagenizing Arf4 into Arf1 we were not causing loss of ERGIC localization indirectly by redistributing the Arf4 receptor to the ER. It is well established that ERGIC structures are retained in cells treated with BFA and Dr. Chun confirmed that the Arf4-GDP receptors still localizes to ERGIC under those conditions (Chun *et al.*, 2008); however the impact of over-expressing the dominant negative Arf1 T31N mutant on ERGIC and the Arf4-GDP receptor remained unknown. To determine whether Arf1 T31N redistributes the Arf4-GDP receptor from punctate ERGIC to diffuse ER, we examined cells co-expressing Arf4 T31N and either Arf1 T31N or Arf5 T31N dominant negative mutants. Results obtained clearly demonstrate that Arf4 T31N remains at puncta in both Arf1 T31N and Arf5 T31N expressing cells (Figure 3.11). These observations demonstrated that mutation of Arf4 into Arf1 would not indirectly cause redistribution of the Arf4-GDP receptor into the ER and established the feasibility of our approach.

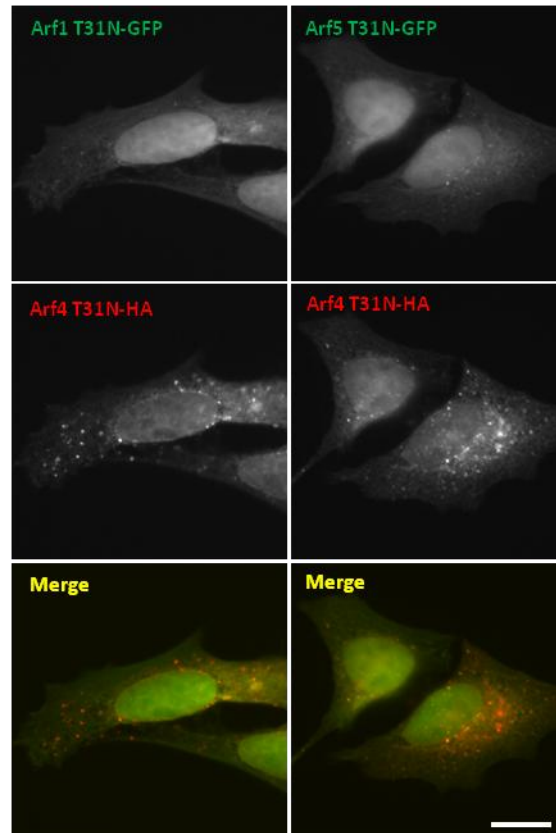


Figure 3.11. Arf4 T31N remains puncta bound in the absence of a Golgi complex

Hela cells were co-transfected with plasmids encoding either Arf4 T31N-GFP and Arf5 T31N-HA or Arf4 T31N-GFP and Arf1 T31N-HA. After 18 hours, cells were fixed and labelled with anti-HA antibodies. Images were acquired by epifluorescence microscopy. Bar, 20 μm .

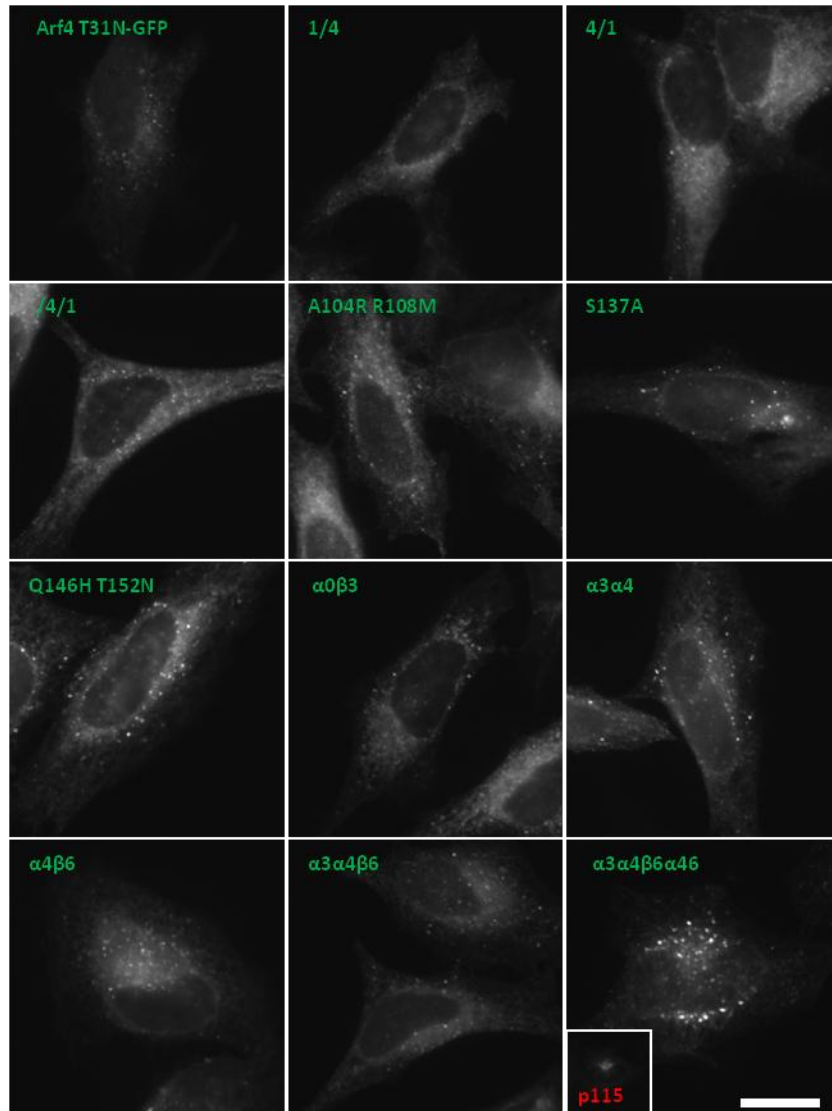


Figure 3.12. Arf4 T31N chimeras remain puncta bound

Hela cells were transfected with the constructs listed in Table 2.3.3 from Materials and Methods. After 18 hours, cell were fixed and labelled for p115 and imaged. Images are representative from two experiments. Inset of p115 staining is only shown for one image but is representative of all images. Every mutant displayed is Arf4 T31N-GFP with indicated mutation. Bar, 20 μ m.

I first modified residues at the N- and C-termini of Arf4 to Arf1 by performing PCR using mutagenic primers. Those residues were tested first because both termini are implicated in membrane binding. The N-terminal amphipathic helix is known to drive membrane association (Haun et al., 1993) and more recently, two residues at the C-terminus of Arf3 were shown to be critical in membrane binding (Manolea et al., 2010). Transiently expressed Arf4 T31N with modified N- (1/4) or C- (1/4) termini still localized to peripheral puncta (Figure 3.12 upper three panels). Therefore, I went on to test internal residues (Figure 3.12). I constructed these single point mutants by site directed mutagenesis. Since all single mutants still accumulated on puncta, I constructed mutants that incorporated combinations of these residues. These mutants were constructed by PCR and site-directed mutagenesis depending on the mutation introduced (Figure 3.12, lower panels). At this point, I have transformed Arf4 T31N almost completely into Arf1 T31N, and the resulting chimeric protein still retained the Arf4 T31N phenotype. Table 2.3.3 from materials and methods lists all the mutants constructed. Figure 3.10 shows a representative image of each mutant constructed. Because all eleven mutants retained the ability to associate with ERGIC, I chose to pursue an alternate avenue summarized in the next section.

3.6 Residues that may play an important role in dominant negative behaviour in Arf1 T31N

Failure to identify Arf4 residues essential for targeting to ERGIC prompted me to examine the basis for another unusual property of Arf4. Mutant Arf4 T31N displays two interesting properties; first it localizes to ERGIC, and second it does not behave as a dominant negative mutant towards the Golgi complex. Transient expression of Arf1 T31N-GFP or Arf5 T31N-GFP resulted in Golgi disruption whereas the Golgi remained intact in Arf4 T31N expressing cells (Figure 3.13). After examining at least 200 cells, most Arf1 T31N and 5 T31N expressing cells displayed a disrupted Golgi whereas Arf4 T31N expressing cells showed virtually no Golgi disruption.

To identify the unique feature(s) of Arf4 T31N that explain why it is not a dominant negative mutant towards the Golgi complex, I examined residues conserved in Arf1 and 5 but different in Arf4 (Figure 3.14A). Two of the five residues identified stood out for a number of reasons. At positions 79 and 113, respectively, Arf4 has lysine and valine residues, whereas both Arf1 and 5 have arginine and glutamate residues. To understand how these residues were orientated in space, we took advantage of Arf1 NMR structure (Bryson et al., 2004) and Arf4 crystal structure (Choe *et al.*, 2005). As Figure 3.14B illustrates, Arf1 residues R⁷⁹ and E¹¹³ appear to form a salt bridge whereas V¹¹³ in Arf4 clearly prevents such interaction.

I mutated Arf4 T31N at the 113 position, exchanging valine for glutamate, expecting to establish a salt bridge with K⁷⁹. To our disappointment, Arf4 T31N

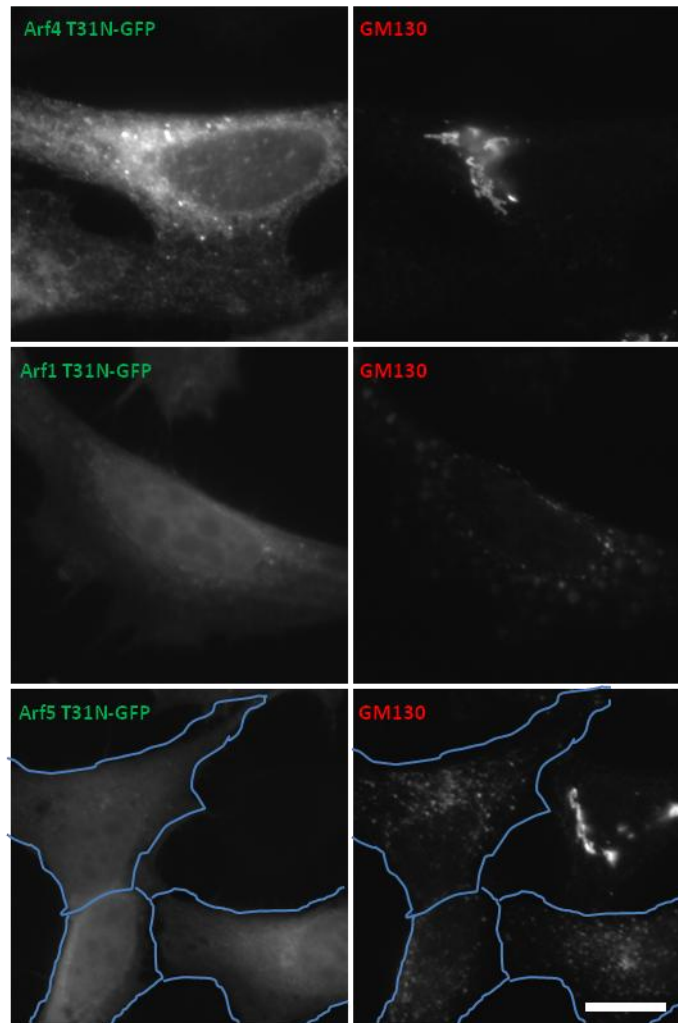


Figure 3.13 Arf1 and 5 T31N disrupt the Golgi complex whereas Arf4 T31N does not

Hela cells were transfected with plasmids encoding Arf1 T31N-GFP, Arf4 T31N-GFP or Arf5 T31N-GFP. 18 hours later, cells were fixed and stained with GM130. Images were acquired using an epifluorescence microscope. Images are representative of at least three separate experiments. Bars, 20 μm .

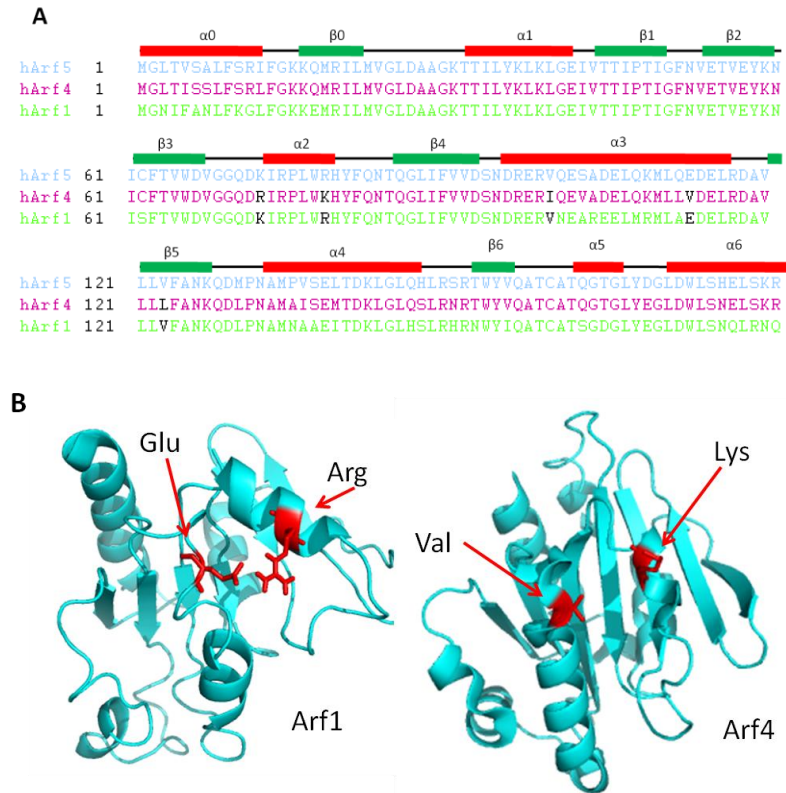


Figure 3.14. 5 residues unique to Arf1 and 5 that may determine whether the T31N mutation yields a dominant negative mutant

A. Alignment of Arf1, 4, and 5 identifies five residues highlighted in black conserved in Arf1 and 5 but divergent in Arf4. **B.** The NMR structure of Arf1 (Bryson *et al.*, 2004) and crystal structure of Arf4 (Choe *et al.*, 2005) have been manipulated in pymol to show a potential Glutamate-Arginine interaction seen in Arf1 absent in Arf4.

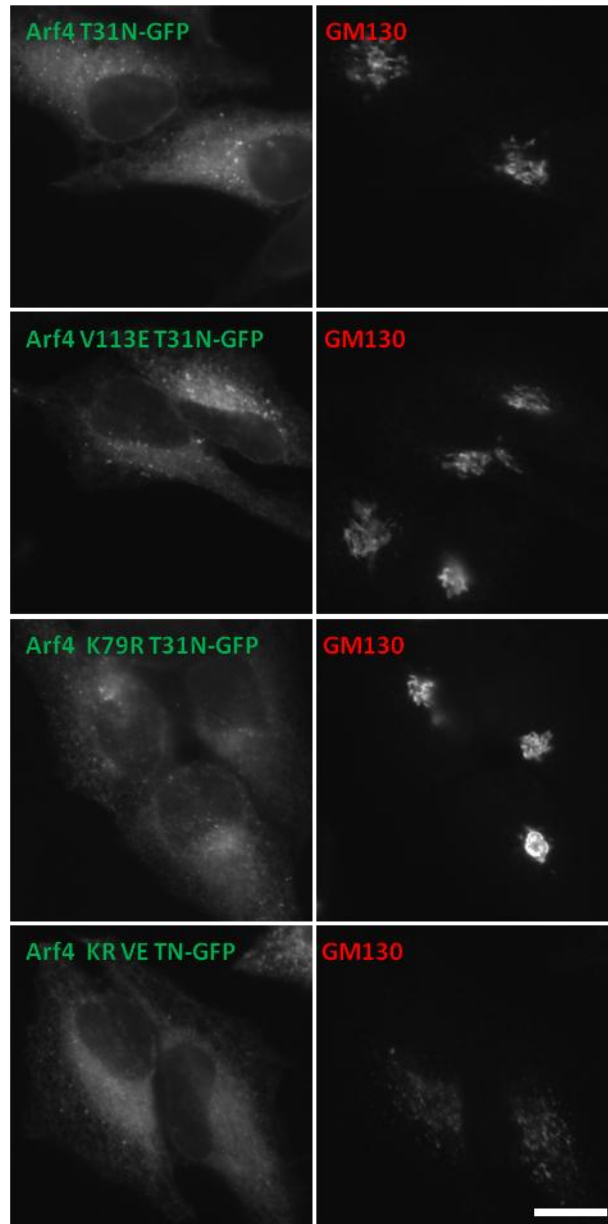


Figure 3.15. Introduction of bridge residues R⁷⁹ and E¹¹³ into Arf4 T31N-GFP yields a dominant negative mutant

Hela cells were transfected with plasmids encoding either Arf4T31N-GFP, or derivatives bearing additional mutations V113E, K79R or K79R V113E. After 18 hours, cells were fixed and labelled for GM130. Images were acquired by epifluorescence microscopy and are representative of at least two experiments. Bars, 20 μ m.

V113E failed to disrupt the Golgi complex as shown in Figure 3.15. Upon further analysis, we concluded that perhaps length was just as important as charge, and that arginine was required at position 79. We first determined whether substituting arginine⁷⁹ for lysine by itself had any impact on the ability of Arf4 T31N to disrupt the Golgi complex. As shown in Figure 3.15, expression of Arf4 T31N K79R failed to disrupt the Golgi complex. In contrast, expression of Arf4-T31N substituted with both Arf1 bridge residues R⁷⁹III E¹¹³ clearly acted as a dominant negative mutant (Figure 3.15). I quantified these results by examining 100 cells per cover slip and scoring cells with either an intact or disrupted Golgi complex (Figure 3.17). Quantification confirmed that Arf4 with the engineered the R⁷⁹III E¹¹³ bridge became a dominant negative mutant.

Building on the results confirmed above, we chose to perform the reciprocal experiment by mutagenizing Arf1 T31N residues involved in the putative salt bridge. As shown in Figure 3.16, a mutant in which R⁷⁹ was changed to K⁷⁹ localized to a juxta-nuclear structure and no longer efficiently disrupted the Golgi complex. Quantitation in Figure 3.17 shows only a partial loss of dominant negative behaviour. More drastic changes to the Arf4 residues K⁷⁹ and V¹¹³ completely abrogated the ability of the Arf1 T31N protein to disrupt the Golgi complex (Figures 3.16 and 3.17). To determine whether the requirement for the R⁷⁹III E¹¹³ pair reflected the importance of a putative ionic bond or a specific requirement for those charges, I swapped the charges of Arf1 T31N from R⁷⁹ to

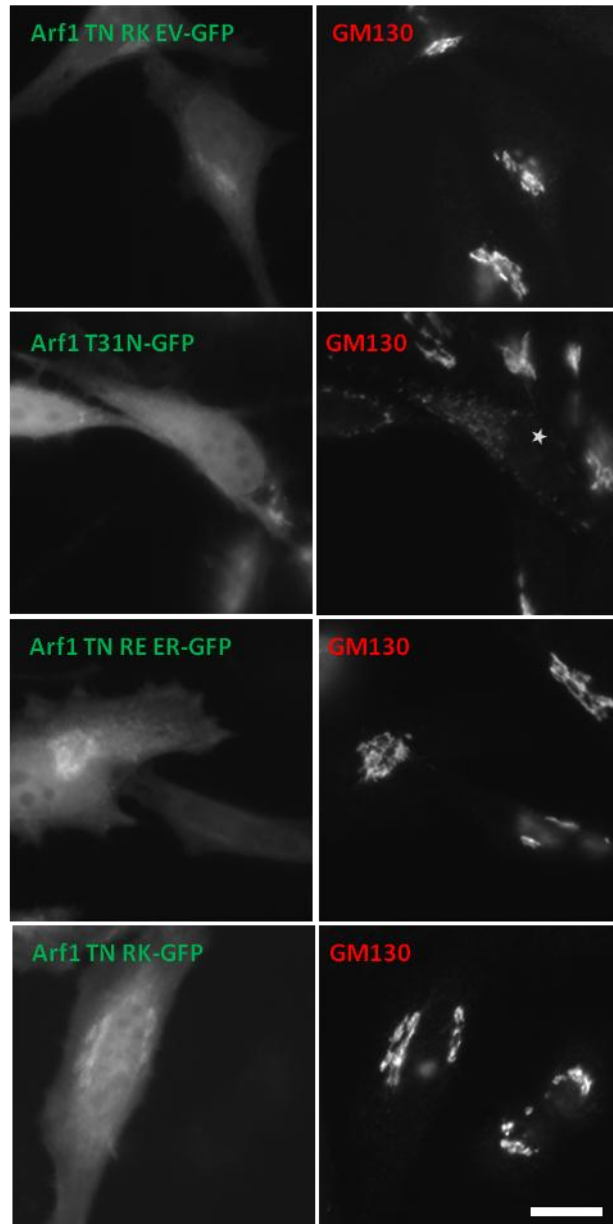


Figure 3.16. Disruption of putative bridge between residues R⁷⁹ and E¹¹³ in Arf1 T31N-GFP reduces dominant negative effect

Hela cells were transfected with plasmid encoding either Arf1 T31N-GFP, or derivatives bearing additional mutations R79E E113R, R79K, or R79K E113V. After 18 hours, cells were fixed and stained for GM130. Images were acquired by epifluorescence microscopy and are representative from a minimum of two separate experiments. Bar, 20 μ m.

Table 3.1. Arf1 and 4 mutants effects on the Golgi complex

List of mutants where the R⁷⁹E¹¹³ interaction has been added or manipulated in Arf4 and manipulated in Arf1.

Arf T31N-GFP mutants	Golgi complex integrity
Arf4	YES
Arf4 V113E	YES
Arf4 K79R	YES
Arf4 K79R V113E	NO
Arf4 K79E V113R	YES
Arf1	NO
Arf1 R79K	YES
Arf1 R79K E113V	YES
Arf1 R79K E113D	YES
Arf1 R79E	YES
Arf1 E113R	YES
Arf1 R79E E113R	YES

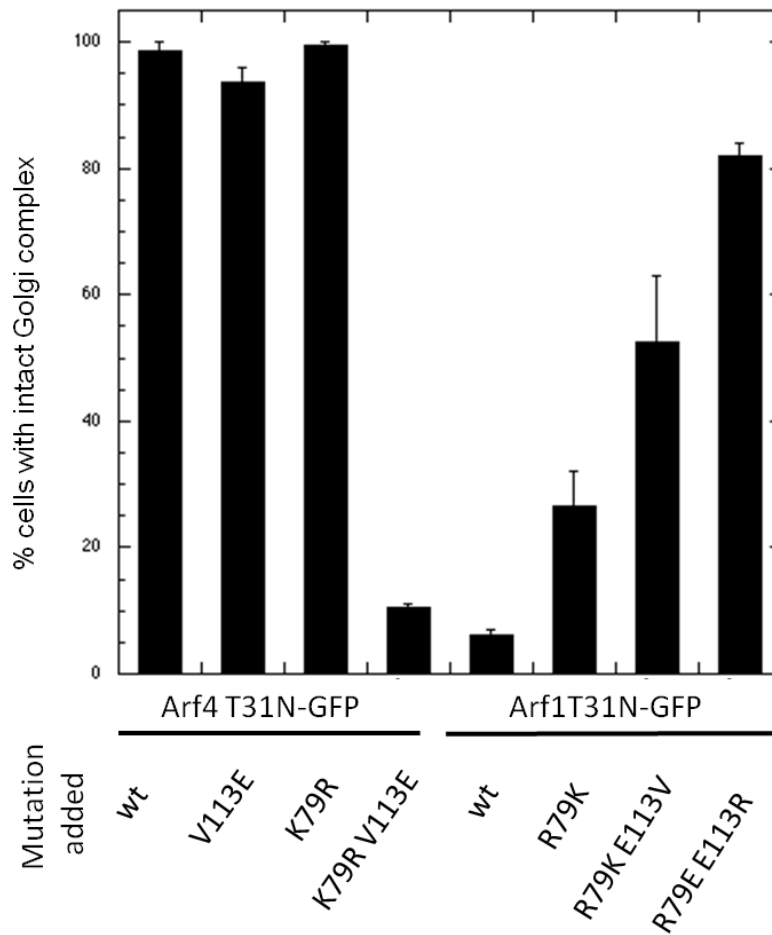


Figure 3.17. Bridge residues R⁷⁹E¹¹³ are important for dominant negative behaviour

Quantitative analysis of dominant negative Arf mutants and their ability to disrupt the Golgi complex. Error bars refer to the average \pm Standard Error (n=100 cell from two separate experiments).

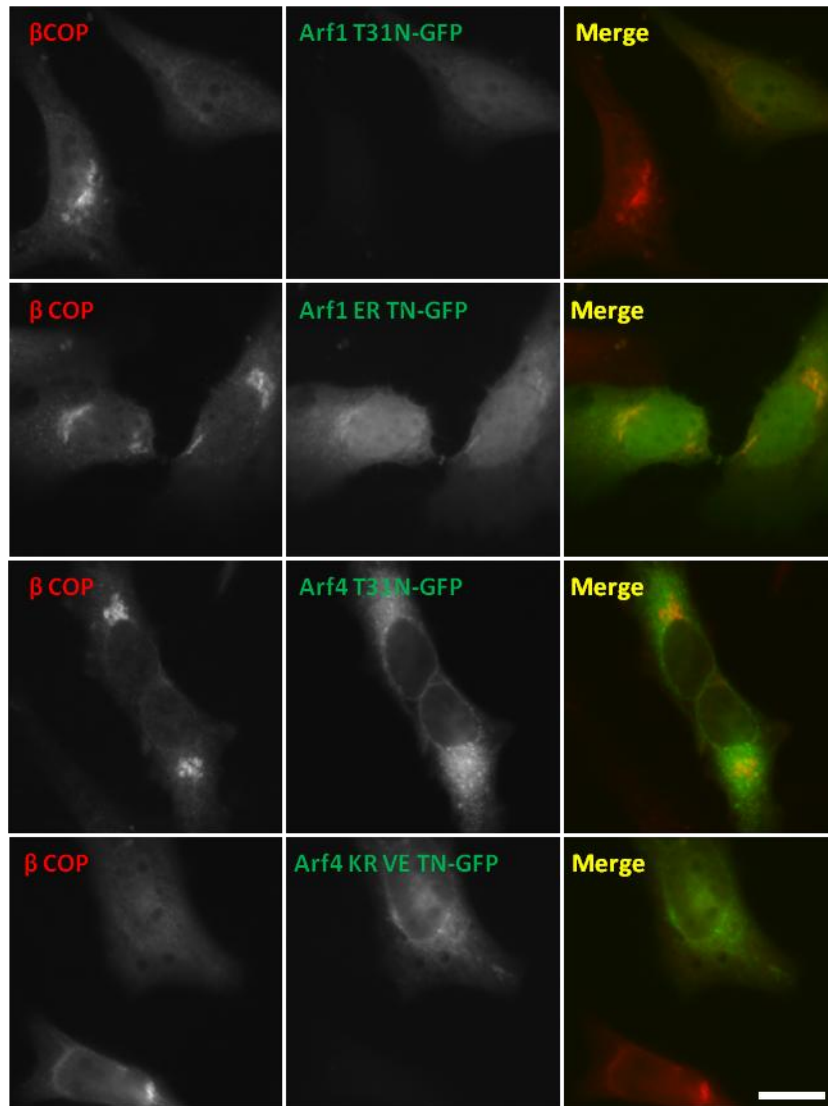


Figure 3.18. β COP staining confirms dominant negative phenotype

Hela cells were transfected with plasmids encoding Arf1 T31N-GFP, Arf4 T31N-GFP, Arf1 E113R T31N-GFP, or Arf4 K79R V113E T31N-GFP. After 18 hours, cells were fixed and labelled for the indicated markers. Images were acquired by epifluorescence microscopy and are representative of two separate experiments. Bars, 20 μ m.

E⁷⁹ and E¹¹³ to R¹¹³ either individually or simultaneously. I found that these mutants were much less effective in redistributing the Golgi complex as can be seen in Figure 3.17. Unfortunately, this result cannot be unambiguously interpreted since we cannot confirm formation of an ionic bridge in this orientation. The nature of the charge at each position appears to also play an important part in dominant negative behaviour towards the Golgi. All mutants constructed and examined for their dominant negative behaviour are summarized in Table 3.1.

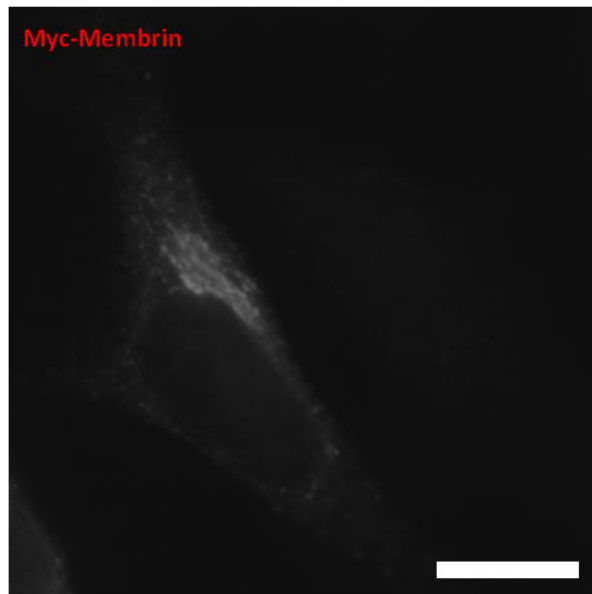
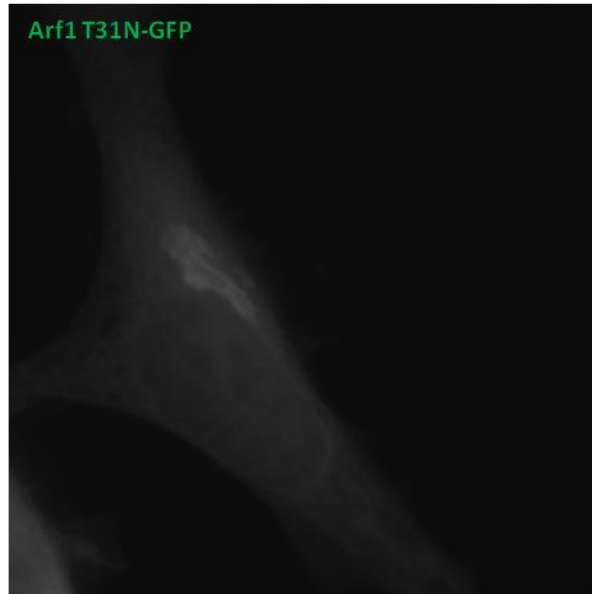
I wanted to confirm that Arf1 T31N with a disrupted R⁷⁹IIIIE¹¹³ bridge not only localized to an intact Golgi but to a functional Golgi as well. Abrogation of the dominant negative behaviour of Arf1 T31N by disrupting the bridge should allow COPI recruitment to the Golgi through endogenous Arf. Conversely, we predicted that Arf4 T31N does not impact the Golgi because it does not disrupt COPI recruitment and that Arf4 mutants that acquired the salt bridge will now prevent COPI recruitment. This would explain the dominant negative effect on the Golgi. For these reasons, I examined the impact of introducing or disrupting the R⁷⁹IIIIE¹¹³ interaction in Arf4 T31N or Arf1 T31N on Golgi complex function. The images shown in Figure 3.18 demonstrate that cells expressing Arf4 K79R V113R T31N no longer maintained a functional Golgi complex positive for COPI. Conversely, cells expressing Arf1 E113R T31N retained a functional Golgi complex positive for COPI.

3.7 Dominant negative behaviour appears as a result from interacting with a protein other than membrin

Interestingly, E¹¹³ resides within the MXXE¹¹³ motif implicated in binding the SNARE membrin at the *cis*-Golgi complex (Honda *et al.*, 2005). On this basis, we hypothesized that trapping membrin is responsible for dominant negative behaviour towards the Golgi and that Arf4 T31N does not act this way because it lacks a salt bridge required for membrin binding. If this is true, over-expression of membrin should trap both dominant negative mutants and abrogate the dominant negative effect. This expectation is based on the observation of Honda *et al.*, (2005) that over-expressed myc-membrin prevents BFA induced redistribution of Arf1. To test this prediction we examined the impact of over-expressing myc-membrin on Golgi distribution in cells co-expressing either Arf1 T31N or Arf4 T31N.

As predicted, over-expression of myc-membrin protected against the Arf1 T31N dominant negative effect because we observed juxta-nuclear myc-membrin positive structure in nearly all co-expressing cells (Figure 3.19A). Not surprisingly, Arf1 T31N also localized to these myc-membrin positive structures. To confirm that Arf1 T31N was bound to membrin positive structures in a GDP bound state, we determined whether retention of the Arf required activation by a GEF. To test this, we treated live cells co-expressing myc-membrin and either wt or mutant Arf1-GFP with BFA, and then imaged Arf distribution as a function

A



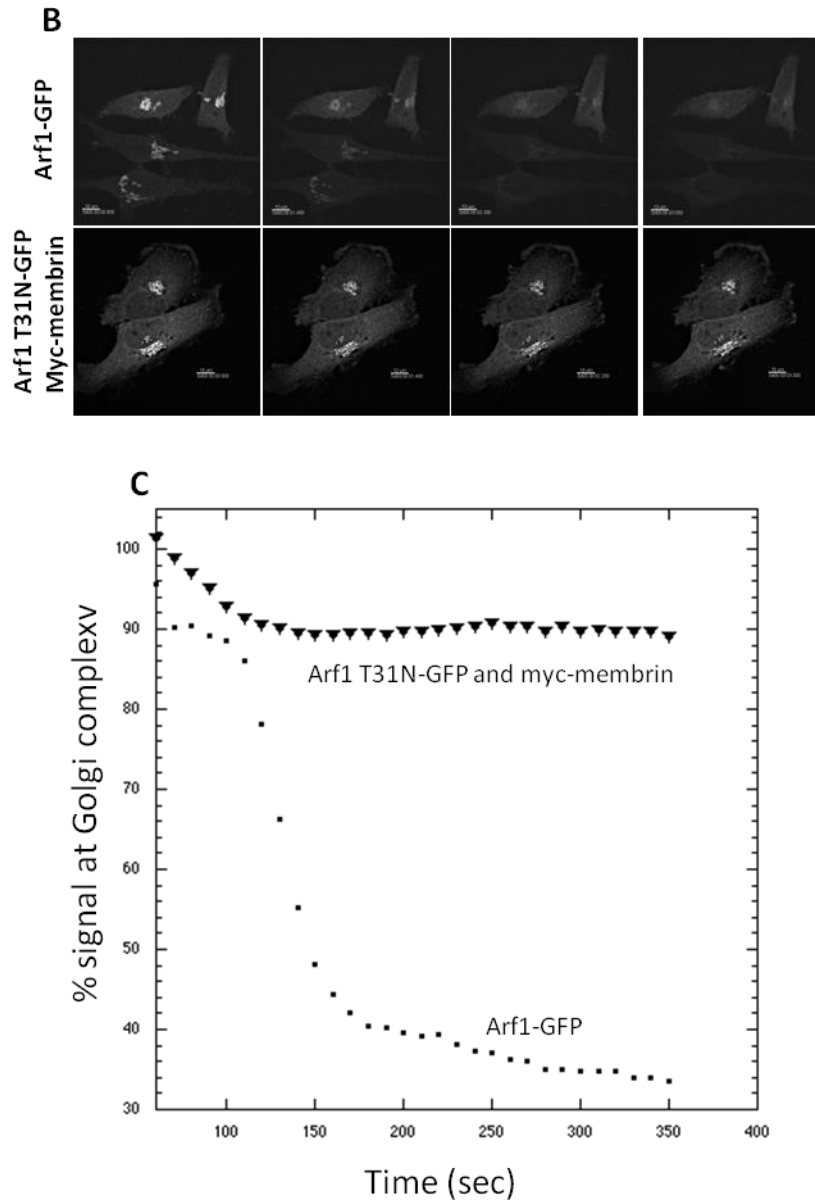


Figure 3.19. Myc-membrin over-expression traps Arf1 T31N in an inactive conformation at the Golgi complex.

A. HeLa cells were co-transfected with plasmids encoding Arf1 T31N-GFP and myc-membrin. After 18 hours, cells were fixed and stained with anti-myc antibodies and imaged by epifluorescence microscopy. **B.** HeLa cells were either singly transfected with plasmid encoding Arf1-GFP or co-transfected with plasmid encoding Arf1 T31N-GFP and myc-membrin. After 18 hours, cells were transferred to the atto chamber and imaged by live cell microscopy. At 60 seconds, BFA (5 $\mu\text{g}/\text{ml}$) was added. Images displayed above are at 60 seconds and at intervals of 80 seconds thereafter. **C.** Quantification of signal loss at the Golgi complex as summarized in Materials and Methods.

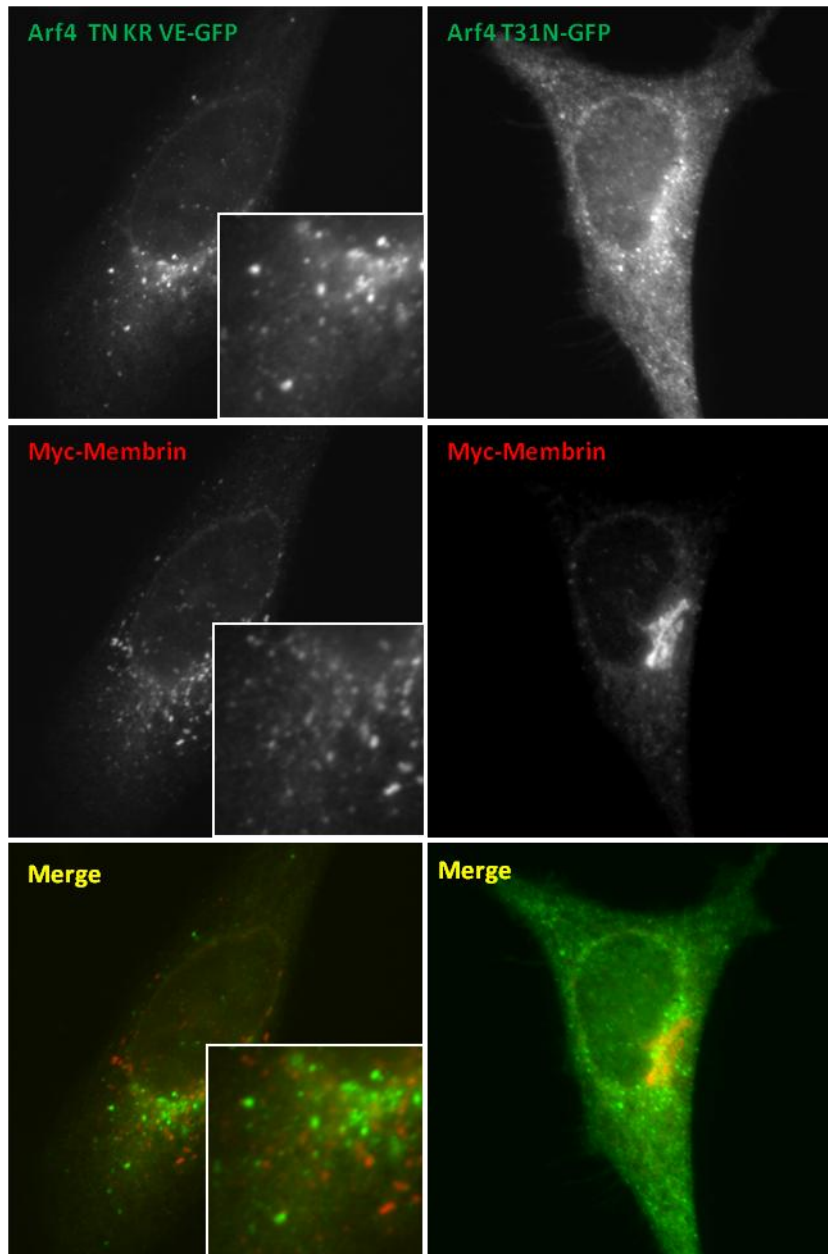


Figure 3.20. Over-expression of myc-membrin fails to rescue the dominant negative effect of Arf4 T31N K79R V113R

Hela cells were co-transfected with plasmids encoding Arf4 T31N K79R V113E-GFP and myc-membrin. After for 18 hours, cells were fixed and labelled with anti-myc antibodies and imaged by epifluorescence microscopy. Bar, 20 μ m. Insets show 2x the magnification of region of interest.

of time. As can be seen in Figure 3.19A, untreated cells co-expressing myc-membrin and Arf1 T31N-GFP show Golgi recruitment; however, after BFA treatment, only Arf1 T31N-GFP remains Golgi localized while Arf1-GFP rapidly redistributed to cytoplasm. These observations demonstrate that Arf1 T31N binds membrin in GDP bound state *in vivo* (Figure 3.19B and C).

To test whether targeting membrin was responsible for the dominant negative effect of Arf4 T31N R79K V113E, we extended this analysis to cells co-expressing Arf4 T31N K79R V113E and myc-membrin. To our surprise, these experiments revealed that myc-membrin did not prevent Arf4 T31N K79R V113E from dispersing the Golgi; instead both proteins appeared in peripheral puncta that likely represented ERGIC (Figure 3.20). This suggests the dominant negative Arf4 T31N K79R V113E does not target membrin but rather another essential component of the transport machinery.

CHAPTER FOUR: DISCUSSION

.

4.1 Summary

The work done on this thesis attempted to further characterize Arf4•GDP at ERGIC. Previously, Dr. Justin Chun had established Arf4•GDP to associate with ERGIC. To extend these results and confirm that Arf4•GDP's association with ERGIC did not result from a tag or mutation artefact, I examined the impact of changing the tag or nature of the mutation on the association of Arf4 with ERGIC. GDP-arrested Arf4 T31N tagged with the smaller HA epitope, Arf4 T31N still associated with peripheral puncta. Even after modifying Arf4 to a "fast cycling" GDP favoured mutant through an N126I mutation, retention to peripheral puncta remained. To further confirm that Arf4•GDP association with ERGIC was real and not a function of aggregation, we examined whether abolishing myristoylation would block Arf4 recruitment to ERGIC. We showed by microscopy and sub-cellular fractionation, that Arf4•GDP membrane recruitment was lost after blocking myristoylation.

After establishing that Arf4•GDP association with ERGIC was real and not a function of aggregation, we focused on indentifying residues in Arf4 that would target it to ERGIC. We identified 17 residues conserved within class II Arfs but absent from Arf1 that could potentially mediate recruitment to ERGIC. Eleven Arf4 T31N mutants were constructed that first focused on the N- and C-terminal helixes separately and together, and then single internal mutations, and finally combinations of these residues. Of the eleven mutants constructed, all remained associated with peripheral puncta.

The “GDP-arrested” Arf4 T31N mutant is not only unique in its association with ERGIC, but also in its failure to act as a dominant negative mutant. Indeed, the T31N mutation transforms Arf1 and Arf5 but not Arf4 into a mutant form that disrupts the Golgi complex. To determine why Arf4 T31N did not disrupt the Golgi, we examined the residues conserved in Arf1 and 5 but divergent in Arf4. Of the five residues identified, two residues in Arf1 and 5 appeared to form a salt bridge absent in Arf4. The Arf1 and 5 residues, R⁷⁹ and E¹¹³ when swapped into Arf4 T31N transformed it into a dominant negative mutant. Furthermore, by changing the length or charge of the putative bridge in Arf1 T31N, the dominant negative behaviour could be reduced significantly. Interestingly, the E¹¹³ of the putative bridge occurred within the MXXE¹¹³ motif of Arf1 found to be important in targeting the *cis*-Golgi through membrin. We hypothesised that the dominant negative properties of Arf1 T31N were through its entrapment of membrin dependent on the R⁷⁹|||E¹¹³ bridge absent in Arf4 T31N. As predicted, over-expression of myc-membrin blocked Arf1 T31N induced redistribution of the Golgi. To our surprise, Arf4 T31N K79R V113E remained a dominant negative in the presence of over-expressed myc-membrin.

4.2 Identifying Arf4 function

It was previously established that single shRNA knock down of individual Arfs had no impact on COP1 localization or on Golgi and endosomal morphology (Volpicelli-Daley et al., 2005). Although, I observed no phenotypic abnormality with the Golgi using siRNAs, more subtle abnormalities associated with vesicle

trafficking could have occurred. By using the temperature sensitive VSVGtsO45-GFP as a cargo molecule, possible defects occurring in traffic from the Golgi to the PM could be observed. At temperatures above 39.5 °C, VSVG-tsO45 cannot fold properly and is retained in the ER; however, once the temperature is lowered to 31.5 °C, the virus glycoprotein is able to travel to the Golgi complex, and then be transported to the plasma membrane (Bergmann, 1989). Arf4 knock down could potentially block/slow down traffic of cargo such as VSVG at ERGIC. Interestingly, there are secretion pathways that altogether bypass the central sorting station, the Golgi (Sannerud et al., 2008). These non-classical pathways are characterized by insensitivity towards BFA, meaning that cargo is trafficked towards the PM regardless of an intact Golgi. Research shows that when VSVG and cholesterol are concentrated at the ERGIC through temperature blocks and then released at permissive temperatures in conjunction with BFA treatment, only cholesterol is transported to the PM (Urbani and Simoni, 1990). I think it would be valuable to look at these kinds of cargo molecules and ask whether or not they are retarded or display an abnormal secretion pathway in cells depleted of Arf4 or expressing a dominant negative Arf4.

Although it was previously established that Arf4•GDP targets to the ERGIC (Chun et al., 2008), its function remains unknown at ERGIC. I have shown that both Arf4 T31N and Arf4 N126I remain puncta bound, and fail to disrupt the Golgi complex. I have also demonstrated that Arf4 siRNA duplexes fail to disrupt the Golgi complex. Identifying changes in the secretion pathway by examining

Golgi morphology was the most obvious and clear assay to do. Unfortunately, the scope of this thesis did not incorporate finer assays to test for defects in the secretory pathway. Some of these tests were previously discussed. Proteins to first examine would be ones that localize to the ERGIC, such as Surf4, p25, p28, p115, YIP1A, Rab1, and Rab2. All of these proteins have implicated at the ERGIC, therefore, may interact in some way with Arf4. Expression of a dominant inactive Arf4 mutant or Arf4 knock down could potentially mislocalize any of these ERGIC localized proteins. Such observations would strongly implicate Arf4 at ERGIC.

4.3 Arf4, a role at the ER?

The data presented in this thesis suggest that Arf4 T31N not only associated with ERGIC but also with the ER. It could be that Arf4•GDP is first recruited at the ER and ERGIC and only activated at the Golgi following transport from the ER and the ERGIC. Even though wt Arf4 expressing cells show no ER localization in the presence or absence of BFA, it would be interesting to test this model. There are two experiments that could help test this model. The first one would take advantage of the dominant negative Sar1 mutant that blocks ER export (Kuge et al., 1994). By co-expressing both Arf4 T31N and Sar1 T39N, I could determine if Arf4 T31N required trafficking out of the ER to associate with the ERGIC. If Arf4 T31N required COPII to exit the ER, Arf4 T31N would lose its peripheral puncta association and become trapped at the ER. To test whether Arf4 activation at the

Golgi required traffic from ERGIC, more elaborate experiments would be required. One approach would involve treating cells expressing Arf4 with the microtubule disrupting drug, nocodazole. The “transport-dependent” model predicts that treatment with nocodazole would rapidly cause loss of Arf4 from the Golgi. We may find that nocodazole treatment has no impact on recruitment and activation of Arf4•GDP at the Golgi. This result would suggest that Arf4•GDP has a unique function at ERGIC.

4.4 Arf4 recruitment to ERGIC

To further characterize Arf4•GDP at ERGIC I examined residues that may play important roles in membrane recruitment. I showed that Arf4 without myristate at the N-terminus failed to recruit to the Golgi complex and ERGIC. Abolishing myristoylation supported Arf4 T31N at the ERGIC to be a biological relevant process and not a function of aggregation. We wanted to further identify the residues responsible in Arf4 recruitment to ERGIC. I identified 17 residues that were conserved in Arf4 and 5 but divergent from Arf1 that may have potential roles in the recruitment of Arf4 to ERGIC. Interestingly, these 17 residues reside in patches on Arf4 that were away from the GEF binding site (Mossessova et al., 1998)(Figure 3.10). It was reasonable to imagine Arf4 binding the ERGIC along this class II specific residue patch through a GDP receptor that would allow presentation of Arf4 to the GEF for activation. Puzzling, my data indicated that all 11 mutants remained punctate bound.

Upon review, we now realize that additional mutants should be investigated to complete the analysis. Although all eleven mutants remained puncta bound, there are two more combinations of mutations that need to be constructed, $\alpha3\alpha4\beta3\beta6\alpha6$ and $\alpha0\alpha3\alpha4\beta3\beta6\alpha6$ (refer to Figure 3.10). Furthermore, there were two residues, one at the Arf4 N-terminus and one at the C-terminus, which we did not include in our mutagenesis. The one at the Arf4 N-terminus, serine⁶, was not mutated to the Arf1 alanine⁶, because both residues were considered to be of similar size. Although serine can be a potential phosphorylation site, Arfs have never been shown to be phosphorylated. The web program NetPhos 2.0 was used to determine if Ser6 was a potential site for phosphorylation. The analysis showed Ser6 to fall below the threshold of phosphorylation. The other Arf4 residue we chose to ignore was positively charged lysine residue at position 179 of the C-terminus. Arf1 has an asparagine at the 179th position, which is not positively charged but polar (Figure 3.14). Recent work in our lab performed by Dr. Florin Manolea (2010) demonstrated that Arf3 localization could be modified by mutating either of two amino acids at its C-terminus. Interestingly, these residues were alanine¹⁷⁴ and lysine¹⁸⁰, very close to the Arf4 residues that were not modified. Further evidence suggests that the C-terminus is critical in membrane recruitment as the last 22 amino acids in Arf1 was shown to bind p23 (Gommel et al., 2001). Construction and characterization of these additional mutants at the N- and C-termini is currently in progress.

4.5 Impact of BFA, Golgicide (GCA), and T31N mutant on VSVG and ERGIC

The Arf1 T31N dominant negative mutant has been shown to redistribute COP1, collapse the Golgi complex to the ER and block trafficking out of the ER (Dascher and Balch, 1994; Ward et al., 2001) just as BFA does (Donaldson et al., 1992; Pelham, 1991). Similarly Exo1 blocks trafficking from the ER and collapses the Golgi complex (Feng et al., 2003; Garcia-Mata et al., 2003). Interestingly, two alternate ways to disrupt the Golgi complex, a GBF1 knock down or treatment with GCA, do not disrupt ER to ERGIC trafficking (Garcia-Mata et al., 2003; Manolea et al., 2008; Saenz et al., 2009). These two ways specifically target the function of GBF1. This begs the question that perhaps Arf1 T31N, BFA, and Exo1 share a target other than GBF1 that disrupts early secretion and/or prevents accumulation of cargo at ERGIC. BFA not only disrupts coat formation, but stimulates the ADP-ribosylation of both BARS-50 and GAPDH (De Matteis et al., 1994). BARS-50 promotes fission of Golgi tubular networks by activating LPA acyltransferase (Weigert et al., 1999). By inhibiting ADP-ribosylation of BARS-50 with dicumarol or Ilimaquinone in the presence of BFA, Golgi collapse can be mitigated, suggesting ADP-ribosylation regulates Golgi structure (Silletta et al., 1999). It could be that Exo1, BFA, and Arf1 T31N target a shared protein mediating directly or indirectly BARS-50 ADP-ribosylation activity. My work suggests the dominant negative effect on the Golgi complex caused by Arf1 T31N or Arf4 K79R V113E T31N is mediated through a protein other than membrin. Using biochemical approaches, it would be interesting to see what proteins

would immunoprecipitate with these dominant negative mutants and if they would have a relationship to the BARS-50 pathway.

4.6 Mechanism for dominant negative effect of “GDP-arrested” Arf mutants

I transformed Arf4 T31N into a dominant negative mutant capable of disrupting the Golgi complex by swapping the K⁷⁹ and V¹¹³ residues for the Arf1 R⁷⁹ and E¹¹³ residues. Upon examination of R⁷⁹ and E¹¹³ residues in Arf1 NMR structure, they appeared to form a salt bridge, whereas the crystal structure of Arf4 failed to show this. My data suggest that indeed there is a salt bridge that impacts dominant negative behaviour in Arf1. The dominant negative effect seems to target something other than membrin. GBF1 would be a likely candidate, however, Arf4 lacks the R⁷⁹|||E¹¹³ bridge but still interacts with GBF1, suggesting that GBF1 is not the target. The salt bridge may serve as a clasp that holds Arf1 and Arf5 in a conformation capable of binding an essential component in protein trafficking. When the bridge is disrupted, the interaction with this essential component is lost.

Future work could potentially identify this protein by biochemical immunoprecipitation assays. Both Arf1 T31N and Arf4 T31N K79R V113E should immunoprecipitate a shared protein absent in Arf4 T31N and Arf1 E113R T31N whereas membrin should immunoprecipitate with both Arf1 mutants but neither of the Arf4 mutants. These assays would further confirm our results that membrin recruits Arf1 but not Arf4 and is not the target of dominant negative

behaviour of the Golgi complex. As I mentioned before, Exo1, BFA, and Arf1 T31N may target a shared component in the secretory pathway, therefore, this component may potentially be the target of Arf1 T31N.

4.7 Arf4•GDP receptor

The work presented by Daniël et al. (2009) showed that Arf4 was BFA resistant in BGМК cells. Initially, we thought that perhaps the BGМК cell line contained mutant Class II Arfs that were resistant to BFA induced inactivation. The other possibility was that Class II Arfs were still sensitive to BFA in BGМК cells, but contained a unique GDP receptor at the Golgi complex. However, after performing our own experiments and treating Arf1 or Arf4 expressing BGМК cells with BFA, this most likely is not the case. Our data demonstrate that Arf4 is BFA sensitive in BGМК cell.

SNAREs and p23 proteins have been shown to interact with Arf1 (Gommel et al., 2001; Honda et al., 2005; Majoul et al., 2001). I used a candidate approach to identify four early secretory pathway SNAREs including Membrin, Rbet1, Sec22, and Syntaxin 5. Unfortunately, all four SNAREs failed to overlap with Arf4 T31N-positive puncta. Unexpectedly, high myc-membrin expression levels forced Arf4 T31N-GFP to co-localize on what appeared to be Golgi fragments. After lowering the amount of myc-membrin expressed, the Golgi complex appeared intact and little co-localization with Arf4 T31N-GFP remained. Possibly, Arf4 has a much lower affinity towards membrin than Arf1, but when the cell becomes saturated

with membrin, the interaction is forced. Although Arf4 T31N did not co-localize with any of the SNAREs at puncta, it appeared to co-localize with sec22b, presumably at ER. Perhaps Arf4 T31N is not a dominant negative of the Golgi complex because it lacks an interaction (R⁷⁹III E¹¹³) that enables it to bind at the Golgi complex and disrupt it. Continuing on with a candidate approach, it would be valuable to examine whether or not the p24 family of proteins interact with Arf4. A number of p24 proteins, p25 and p28, have both been shown to localize to ERGIC (Eva et al., ; Mitrovic et al., 2008). A proteomics approach would be another way to identify an Arf4•GDP receptor. By using a triple HA tagged Arf4 T31N and Arf4 G2A T31N (negative control) in an immunoprecipitation assay, we could potentially identify an interacting protein of Arf4•GDP.

CHAPTER 5: REFERENCES

- Alvarez, C., H. Fujita, A. Hubbard, and E. Sztul. 1999. ER to Golgi transport: Requirement for p115 at a pre-Golgi VTC stage. *J Cell Biol.* 147:1205-22.
- Anantharaman, V., and L. Aravind. 2002. The GOLD domain, a novel protein module involved in Golgi function and secretion. *Genome Biol.* 3:research0023.1-research0023.7.
- Antonny, B., D. Madden, S. Hamamoto, L. Orci, and R. Schekman. 2001. Dynamics of the COPII coat with GTP and stable analogues. *Nat Cell Biol.* 3:531-7.
- Aoe, T., E. Cukierman, A. Lee, D. Cassel, P.J. Peters, and V.W. Hsu. 1997. The KDEL receptor, ERD2, regulates intracellular traffic by recruiting a GTPase-activating protein for ARF1. *Embo J.* 16:7305-16.
- Appenzeller-Herzog, C., and H.P. Hauri. 2006. The ER-Golgi intermediate compartment (ERGIC): in search of its identity and function. *J Cell Sci.* 119:2173-83.
- Appenzeller, C., H. Andersson, F. Kappeler, and H.P. Hauri. 1999. The lectin ERGIC-53 is a cargo transport receptor for glycoproteins. *Nat Cell Biol.* 1:330-4.
- Barlowe, C., and R. Schekman. 1993. SEC12 encodes a guanine-nucleotide-exchange factor essential for transport vesicle budding from the ER. *Nature.* 365:347-349.
- Ben-Tekaya, H., K. Miura, R. Pepperkok, and H.P. Hauri. 2005. Live imaging of bidirectional traffic from the ERGIC. *J Cell Sci.* 118:357-67.
- Bergmann, J.E. 1989. Using temperature-sensitive mutants of VSV to study membrane protein biogenesis. *Methods Cell Biol.* 32:85-110.
- Béthune, J., F. Wieland, and J. Moelleken. 2006. COPI-mediated Transport. *J Mem Biol.* 211:65-79.
- Blum, R., F. Pfeiffer, P. Feick, W. Nastainczyk, B. Kohler, K.H. Schafer, and M. Chabre. 1999. Intracellular localization and in vivo trafficking of p24A and p23. *J Cell Sci.* 112:537-48.
- Boman, A.L., and R.A. Kahn. 1995. Arf proteins: the membrane traffic police? *Trends Biochem Sci.* 20:147-50.
- Bonifacino, J.S., and B.S. Glick. 2004. The mechanisms of vesicle budding and fusion. *Cell.* 116:153-66.
- Bonifacino, J.S., and J. Lippincott-Schwartz. 2003. Coat proteins: shaping membrane transport. *Nat Rev Mol Cell Biol.* 4:409-14.
- Boulay, P.L., M. Cotton, P. Melancon, and A. Claing. 2008. ADP-ribosylation factor 1 controls the activation of the phosphatidylinositol 3-kinase pathway to regulate epidermal growth factor-dependent growth and migration of breast cancer cells. *J Biol Chem.* 283:36425-34.
- Bremser, M., W. Nickel, M. Schweikert, M. Ravazzola, M. Amherdt, C.A. Hughes, T.H. Sollner, J.E. Rothman, and F.T. Wieland. 1999. Coupling of coat assembly and vesicle budding to packaging of putative cargo receptors. *Cell.* 96:495-506.
- Casanova, J.E. 2007. Regulation of Arf activation: the Sec7 family of guanine nucleotide exchange factors. *Traffic.* 8:1476-85.
- Cavenagh, M.M., J.A. Whitney, K. Carroll, C. Zhang, A.L. Boman, A.G. Rosenwald, I. Melman, and R.A. Kahn. 1996. Intracellular distribution of ARF proteins in mammalian cells. ARF6 is uniquely localized to the plasma membrane. *J. Biol Chem.* 271:21786-84.
- Chein-Fuang, H., and C. Nin-Nin. 2000. Disrupting the geranylgeranylation at the C-termini of the shrimp Ras by depriving guanine nucleotide binding at the N-terminal. *J Exp Zool.* 286:441-449.

- Cherfils, J., and P. Melançon. 2005. On the action of Brefeldin A on Sec7-stimulated membrane-recruitment and GDP/GTP exchange of Arf proteins. *Biochem Soc Trans.* 33:635-8.
- Chun, J., Z. Shapovalova, S.Y. Dejgaard, J.F. Presley, and P. Melancon. 2008. Characterization of class I and II ADP-ribosylation factors (Arfs) in live cells: GDP-bound class II Arfs associate with the ER-Golgi intermediate compartment independently of GBF1. *Mol Biol Cell.* 19:3488-500.
- Ciufo, L.F., and A. Boyd. 2000. Identification of a luminal sequence specifying the assembly of Emp24p into p24 complexes in the yeast secretory pathway. *J Biol Chem.* 275:8382-8388.
- Cohen, L.A., A. Honda, P. Varnai, F.D. Brown, T. Balla, and J.G. Donaldson. 2007. Active Arf6 recruits ARNO/cytohesin GEFs to the PM by binding their PH domains. *Mol Biol Cell.* 18:2244-53.
- Connerly, P.L., M. Esaki, E.A. Montegna, D.E. Strongin, S. Levi, J. Soderholm, and B.S. Glick. 2005. Sec16 is a determinant of transitional ER organization. *Curr Biol.* 15:1439-47.
- Cool, R.H., G. Schmidt, C.U. Lenzen, H. Prinz, D. Vogt, and A. Wittinghofer. 1999. The Ras Mutant D119N Is Both Dominant Negative and Activated. *Mol Cell Bio.* 19:6297-6305.
- Cosson, P., and F. Letourneur. 1994. Coatamer interaction with di-lysine endoplasmic reticulum retention motifs. *Science.* 263:1629-31.
- D'Souza-Schorey, C., G. Li, M.I. Colombo, and P.D. Stahl. 1995. A regulatory role for ARF6 in receptor-mediated endocytosis. *Science.* 267:1175-8.
- Daniël, D., H.W.L. Kjerstin, H.J.v.D. Sander, M.T.v.D. Michiel, W. Roy, M. Fabrizio de, W. Els, and J.M.v.K. Frank. 2009. Differential Membrane Association Properties and Regulation of Class I and Class II Arfs. *Traffic.* 10:316-323.
- Dascher, C., and W.E. Balch. 1994. Dominant inhibitory mutants of ARF1 block endoplasmic reticulum to Golgi transport and trigger disassembly of the Golgi apparatus. *J Biol Chem.* 269:1437-48.
- De Matteis, M., A. Godi, and D. Corda. 2002. Phosphoinositides and the golgi complex. *Curr Opin Cell Biol.* 14:434-47.
- De Matteis, M.A., M. Di Girolamo, A. Colanzi, M. Pallas, G. Di Tullio, L.J. McDonald, J. Moss, G. Santini, S. Bannykh, D. Corda, and a. et. 1994. Stimulation of endogenous ADP-ribosylation by brefeldin A. *Proc Natl Acad Sci U S A.* 91:1114-8.
- Deng, Y., M.-P. Golinelli-Cohen, E. Smirnova, and C.L. Jackson. 2009. A COPI coat subunit interacts directly with an early-Golgi localized Arf exchange factor. *EMBO Rep.* 10:58-64.
- Denzel, A., F. Otto, A. Girod, R. Pepperkok, R. Watson, I. Rosewell, J.J. Bergeron, R.C. Solari, and M.J. Owen. 2000. The p24 family member p23 is required for early embryonic development. *Curr Biol.* 10:55-8.
- Deretic, D., A.H. Williams, N. Ransom, V. Morel, P.A. Hargrave, and A. Arendt. 2005. Rhodopsin C terminus, the site of mutations causing retinal disease, regulates trafficking by binding to ADP-ribosylation factor 4 (ARF4). *Proc Natl Acad Sci U S A.* 102:3301-6.
- Derrien, V., C. Couillault, M. Franco, S. Martineau, P. Montcourrier, R. Houlgatte, and P. Chavrier. 2002. A conserved C-terminal domain of EFA6-family ARF6-guanine

- nucleotide exchange factors induces lengthening of microvilli-like membrane protrusions. *J Cell Sci.* 115:2867-79.
- Donaldson, J.G., D. Finazzi, and R.D. Klausner. 1992. Brefeldin A inhibits Golgi membrane catalyzed exchange of guanine nucleotide onto ARF protein. *Nature.* 360:350-352.
- Espenshade, P., R.E. Gimeno, E. Holzmacher, P. Teung, and C.A. Kaiser. 1995. Yeast SEC16 gene encodes a multidomain vesicle coat protein that interacts with Sec23p. *J Cell Biol.* 131:311-24.
- Eva, K., B. Carine, W. Lorenz, M. Sandra, H. Regula, and H. Hans-Peter. p28, a novel ERGIC/ cis Golgi protein, required for Golgi ribbon formation. *Traffic.* 11:70-89.
- Fasshauer, D., R.B. Sutton, A.T. Brunger, and R. Jahn. 1998. Conserved structural features of the synaptic fusion complex: SNARE proteins reclassified as Q- and R-SNAREs. Vol. 95. 15781-15786.
- Feig, L.A., and G.M. Cooper. 1988. Inhibition of NIH 3T3 cell proliferation by a mutant ras protein with preferential affinity for GDP. *Mol Cell Biol.* 8:3235-3243.
- Feng, Y., S. Yu, T.K. Lasell, A.P. Jadhav, E. Macia, P. Chardin, P. Melançon, M. Roth, T. Mitchison, and T. Kirchhausen. 2003. Exo1: a new chemical inhibitor of the exocytic pathway. *Proc Natl Acad Sci U S A.* 100:6469-74.
- Frank, S., S. Upender, S.H. Hansen, and J.E. Casanova. 1998. ARNO is a guanine nucleotide exchange factor for ADP-ribosylation factor 6. *J Biol Chem.* 273:23-7.
- Fromme, J.C., and R. Schekman. 2005. COPII-coated vesicles: flexible enough for large cargo? *Curr Opin Cell Biol.* 17:345-52.
- Garcia-Mata, R., T. Szul, C. Alvarez, and E. Sztul. 2003. ADP-ribosylation factor/COPI-dependent events at the endoplasmic reticulum-Golgi interface are regulated by the guanine nucleotide exchange factor GBF1. *Mol Biol Cell.* 14:2250-61.
- Glick, B.S., and V. Malhotra. 1998. The curious status of the Golgi apparatus. *Cell.* 95:883-9.
- Goldberg, J. 1998. Structural basis for activation of ARF GTPase: mechanisms of guanine nucleotide exchange and GTP-myristoyl switching. *Cell.* 95:237-48.
- Goldberg, J. 2000. Decoding of sorting signals by coatomer through a GTPase switch in the COPI coat complex. *Cell.* 100:671-9.
- Gommel, D.U., A.R. Memon, A. Heiss, F. Lottspeich, J. Pfannstiel, J. Lechner, C. Reinhard, J.B. Helms, W. Nickel, and F.T. Wieland. 2001. Recruitment to Golgi membranes of ADP-ribosylation factor 1 is mediated by the cytoplasmic domain of p23. *Embo J.* 20:6751-60.
- Hara-Kuge, S., O. Kuge, L. Orci, M. Amherdt, M. Ravazzola, F.T. Wieland, and J.E. Rothman. 1994. En bloc incorporation of coatomer subunits during the assembly of COP-coated vesicles. *J Cell Biol.* 124:883-92.
- Haun, R.S., S.C. Tsai, R. Adamik, J. Moss, and M. Vaughan. 1993. Effect of myristoylation on GTP-dependent binding of ADP-ribosylation factor to Golgi. *J Biol Chem.* 268:7064-7068.
- Hauri, H.P., F. Kappeler, H. Andersson, and C. Appenzeller. 2000. ERGIC-53 and traffic in the secretory pathway. *J Cell Sci.* 113(Pt 4):587-96.
- Hay, J.C., D.S. Chao, C.S. Kuo, and R.H. Scheller. 1997. Protein Interactions Regulating Vesicle Transport between the Endoplasmic Reticulum and Golgi Apparatus in Mammalian Cells. *Cell.* 89:149-158.
- Hay, J.C., H. Hirling, and R.H. Scheller. 1996. Mammalian vesicle trafficking proteins of the endoplasmic reticulum and Golgi apparatus. *J Biol Chem.* 271:5671-9.

- Hay, J.C., J. Klumperman, V. Oorschot, M. Steegmaier, C.S. Kuo, and R.H. Scheller. 1998. Localization, Dynamics, and Protein Interactions Reveal Distinct Roles for ER and Golgi SNAREs. *J Cell Biol.* 141:1489-502.
- Holloway, Z.G., R. Grabski, T. Szul, M.L. Styers, J.A. Coventry, A.P. Monaco, and E. Sztul. 2007. Activation of ADP-ribosylation factor regulates biogenesis of the ATP7A-containing trans-Golgi network compartment and its Cu-induced trafficking. *AJP Cell Phys.* 293:C1753-1767.
- Honda, A., O.S. Al-Awar, J.C. Hay, and J.G. Donaldson. 2005. Targeting of Arf-1 to the early Golgi by membrin, an ER-Golgi SNARE. *J Cell Biol.* 168:1039-51.
- Hong, W. 2005. SNAREs and traffic. *Biochim Biophys Acta.* 1744:120-44.
- Jackson, T.R., F.D. Brown, Z. Nie, K. Miura, L. Foroni, J. Sun, V.W. Hsu, J.G. Donaldson, and P.A. Randazzo. 2000. Acaps Are Arf6 Gtpase-Activating Proteins That Function in the Cell Periphery. *J Cell Biol.* 151:627-638.
- Jenne, N., K. Frey, B. Brugger, and F.T. Wieland. 2002. Oligomeric state and stoichiometry of p24 proteins in the early secretory pathway. *J Biol Chem.* 277:46504-11.
- Kano, F., S. Yamauchi, Y. Yoshida, M. Watanabe-Takahashi, K. Nishikawa, N. Nakamura, and M. Murata. 2009. Yip1A regulates the COPI-independent retrograde transport from the Golgi complex to the ER. *J Cell Sci.* 122:2218-2227.
- Kappeler, F., D.R. Klopfenstein, M. Foguet, J.P. Paccaud, and H.P. Hauri. 1997. The recycling of ERGIC-53 in the early secretory pathway. ERGIC-53 carries a cytosolic endoplasmic reticulum-exit determinant interacting with COPII. *J Biol Chem.* 272:31801-8.
- Klarlund, J.K., A. Guilherme, J.J. Holik, J.V. Virbasius, A. Chawla, and M.P. Czech. 1997. Signaling by phosphoinositide-3,4,5-trisphosphate through proteins containing pleckstrin and Sec7 homology domains. *Science.* 275:1927-30.
- Kuge, O., C. Dascher, L. Orci, T. Rowe, M. Amherdt, H. Plutner, M. Ravazzola, G. Tanigawa, J.E. Rothman, and W.E. Balch. 1994. Sar1 promotes vesicle budding from the endoplasmic reticulum but not Golgi compartments. *J Cell Biol.* 125:51-65.
- Lederkremer, G.Z., Y. Cheng, B.M. Petre, E. Vogan, S. Springer, R. Schekman, T. Walz, and T. Kirchhausen. 2001. Structure of the Sec23p/24p and Sec13p/31p complexes of COPII. *Proc Natl Acad Sci U S A.* 98:10704-10709.
- Linstedt, A.D., and H.P. Hauri. 1993. Giantin, a novel conserved Golgi membrane protein containing a cytoplasmic domain of at least 350 kDa. *Mol Biol Cell.* 4:679-93.
- Lippincott-Schwartz, J., and W. Liu. 2003. Membrane trafficking: coat control by curvature. *Nature.* 426:507-8.
- Lippincott-Schwartz, J., L.C. Yuan, J.S. Bonifacino, and R.D. Klausner. 1989. Rapid redistribution of Golgi proteins into the ER in cells treated with brefeldin A: evidence for membrane cycling from Golgi to ER. *Cell.* 56:801-13.
- Losev, E., C.A. Reinke, J. Jellen, D.E. Strongin, B.J. Bevis, and B.S. Glick. 2006. Golgi maturation visualized in living yeast. *Nature.* 441:1002-6.
- Luton, F., S. Klein, J.P. Chauvin, A. Le Bivic, S. Bourgoin, M. Franco, and P. Chardin. 2004. EFA6, exchange factor for ARF6, regulates the actin cytoskeleton and associated tight junction in response to E-cadherin engagement. *Mol Biol Cell.* 15:1134-45.
- Macia, E., F. Luton, M. Partisani, J. Cherfils, P. Chardin, and M. Franco. 2004. The GDP-bound form of Arf6 is located at the plasma membrane. *J Cell Sci.* 117:2389-98.

- Majoul, I., M. Straub, S.W. Hell, R. Duden, and H.-D. Soling. 2001. KDEL-cargo regulates interactions between proteins involved in COPI vesicle traffic: Measurements in living cells using FRET. *Dev Cell*. 1:139-145.
- Mancias, J.D., and J. Goldberg. 2008. Structural basis of cargo membrane protein discrimination by the human COPII coat machinery. *EMBO J*. 27:2918-2928.
- Manolea, F., J. Chun, I. Clarke, D. Chen, N. Summerfeldt, J. Dacks, and P. Melançon. 2010. Arf3 is activated selectively by the large guanine nucleotide exchange factors BIGs at the trans-Golgi network. *Mol Biol Cell*. In press:In press
- Manolea, F., A. Claude, J. Chun, J. Rosas, and P. Melançon. 2008. Distinct functions for Arf guanine nucleotide exchange factors at the Golgi complex: GBF1 and BIGs are required for assembly and maintenance of the Golgi stack and trans-Golgi network, respectively. *Mol Biol Cell*. 19:523-35.
- Mansour, S.J., J. Skaug, X.H. Zhao, J. Giordano, S.W. Scherer, and P. Melançon. 1999. p200 ARF-GEP1: a Golgi-localized guanine nucleotide exchange protein whose Sec7 domain is targeted by the drug brefeldin A. *Proc Natl Acad Sci U S A*. 96:7968-73.
- Marie, M., H.A. Dale, R. Sannerud, and J. Saraste. 2009. The function of the intermediate compartment in pre-Golgi trafficking involves its stable connection with the centrosome. *Mol Biol Cell*. 20:4458-4470.
- Matsuoka, K., L. Orci, M. Amherdt, S.Y. Bednarek, S. Hamamoto, R. Schekman, and T. Yeung. 1998. COPII-coated vesicle formation reconstituted with purified coat proteins and chemically defined liposomes. *Cell*. 93:263-75.
- Matsuura-Tokita, K., M. Takeuchi, A. Ichihara, K. Mikuriya, and A. Nakano. 2006. Live imaging of yeast Golgi cisternal maturation. *Nature*. 441:1007-10.
- Mazelova, J., L. Astuto-Gribble, H. Inoue, B.M. Tam, E. Schonteich, R. Prekeris, O.L. Moritz, P.A. Randazzo, and D. Deretic. 2009. Ciliary targeting motif VxPx directs assembly of a trafficking module through Arf4. *EMBO J*. 28:183-192.
- Miller, E.A., T.H. Beilharz, P.N. Malkus, M.C. Lee, S. Hamamoto, L. Orci, and R. Schekman. 2003. Multiple cargo binding sites on the COPII subunit Sec24p ensure capture of diverse membrane proteins into transport vesicles. *Cell*. 114:497-509.
- Mitrovic, S., H. Ben-Tekaya, E. Koezler, J. Gruenberg, and H.P. Hauri. 2008. The cargo receptors Surf4, Endoplasmic Reticulum-Golgi intermediate compartment (ERGIC)-53, and p25 are required to maintain the architecture of ERGIC and Golgi. *Mol Biol Cell*. 19:1976-90.
- Mogelsvang, S., B.J. Marsh, M.S. Ladinsky, and K.E. Howell. 2004. Predicting function from structure: 3D structure studies of the mammalian Golgi complex. *Traffic*. 5:338-45.
- Mossessova, E., L.C. Bickford, and J. Goldberg. 2003. SNARE selectivity of the COPII coat. *Cell*. 114:483-95.
- Mossessova, E., J.M. Gulbis, and J. Goldberg. 1998. Structure of the guanine nucleotide exchange factor Sec7 domain of human arno and analysis of the interaction with ARF GTPase. *Cell*. 92:415-23.
- Nakamura, N., C. Rabouille, R. Watson, T. Nilsson, N. Hui, P. Slusarewicz, T.E. Kreis, and G. Warren. 1995. Characterization of a cis-Golgi matrix protein, GM130. *J Cell Biol*. 131:1715-26.
- Nakano, A., and M. Muramatsu. 1989. A novel GTP-binding protein, Sar1p, is involved in transport from the endoplasmic reticulum to the Golgi apparatus. *J Cell Biol*. 109:2677-2691.

- Nelson, D.S., C. Alvarez, Y.S. Gao, R. Garcia-Mata, E. Fialkowski, and E. Sztul. 1998. The membrane transport factor TAP/p115 cycles between the Golgi and earlier secretory compartments and contains distinct domains required for its localization and function. *J Cell Biol.* 143:319-31.
- Nishimura, N., and W.E. Balch. 1997. A di-acidic signal required for selective export from the endoplasmic reticulum. *Science.* 277:556-8.
- Orci, L., M. Ravazzola, P. Meda, C. Holcomb, H.P. Moore, L. Hicke, and R. Schekman. 1991. Mammalian Sec23p homologue is restricted to the endoplasmic reticulum transitional cytoplasm. *Proc Natl Acad Sci U S A.* 88:8611-5.
- Palmer, D.J., J.B. Helms, C.J.M. Beckers, L. Orci, and J.E. Rothman. 1993. Binding of coatamer to Golgi membranes requires ADP-ribosylation. *J Biol Chem.* 268:12083-12089.
- Pasqualato, S., L. Renault, and J. Cherfils. 2002. Arf, Arl, Arp and Sar proteins: a family of GTP-binding proteins with a structural device for 'front-back' communication. *EMBO Rep.* 3:1035-41.
- Pelham, H.R. 1991. Recycling of proteins between the endoplasmic reticulum and Golgi complex. *Curr Opin Cell Biol.* 3:585-91.
- Peyroche, A., B. Antony, S. Robineau, J. Acker, J. Cherfils, and C.L. Jackson. 1999. Brefeldin A acts to stabilize an abortive ARF-GDP-Sec7 domain protein complex: involvement of specific residues of the Sec7 domain. *Mol Cell.* 3:275-85.
- Presley, J.F., N.B. Cole, T.A. Schroer, K. Hirschberg, K.J. Zaal, and J. Lippincott-Schwartz. 1997. ER-to-Golgi transport visualized in living cells. *Nature.* 389:81-5.
- Puthenveedu, M.A., and A.D. Linstedt. 2005. Subcompartmentalizing the Golgi apparatus. *Curr Opin Cell Biol.* 17:369-75.
- Rambourg, A., and Y. Clermont. 1990. Three-dimensional electron microscopy: structure of the Golgi apparatus. *Eur J Cell Biol.* 51:189-200.
- Randazzo, P.A. 1997. Resolution of two ADP-ribosylation factor 1 GTPase-activating proteins from rat liver. *Biochem J.* 324:413-9.
- Randazzo, P.A., and D.S. Hirsch. 2004. Arf GAPs: multifunctional proteins that regulate membrane traffic and actin remodelling. *Cell Signal.* 16:401-13.
- Rein, U., U. Andag, R. Duden, H.D. Schmitt, and A. Spang. 2002. ARF-GAP-mediated interaction between the ER-Golgi v-SNAREs and the COPI coat. *J Cell Biol.* 157:395-404.
- Renault, L., B. Guibert, and J. Cherfils. 2003. Structural snapshots of the mechanism and inhibition of a guanine nucleotide exchange factor. *Nature.* 426:525-30.
- Robineau, S., M. Chabre, and B. Antony. 2000. Binding site of brefeldin A at the interface between the small G protein ADP-ribosylation factor 1 (ARF1) and the nucleotide-exchange factor Sec7 domain. *Proc Natl Acad Sci U S A.* 97:9913-8.
- Rodriguez-Boulant, E., and A. Musch. 2005. Protein sorting in the Golgi complex: shifting paradigms. *Biochem Biophys Acta.* 1744:455-64.
- Rojo, M., R. Pepperkok, G. Emery, R. Kellner, E. Stang, R.G. Parton, and J. Gruenberg. 1997. Involvement of the Transmembrane Protein p23 in Biosynthetic Protein Transport. *J Cell Biol.* 139:1119-1135.
- Saenz, J.B., W.J. Sun, J.W. Chang, J. Li, B. Bursulaya, N.S. Gray, and D.B. Haslam. 2009. Golgicide A reveals essential roles for GBF1 in Golgi assembly and function. *Nat Chem Biol.*

- Saraste, J., H.A. Dale, S. Bazzocco, and M. Marie. 2009. Emerging new roles of the pre-Golgi intermediate compartment in biosynthetic-secretory trafficking. *FEBS Letters*. 583:3804-3810.
- Sato, K., and A. Nakano. 2007. Mechanisms of COPII vesicle formation and protein sorting. *FEBS Lett*. 581:2076-82.
- Schweizer, A., J.A. Fransen, T. Bachi, L. Ginsel, and H.P. Hauri. 1988. Identification, by a monoclonal antibody, of a 53-kD protein associated with a tubulo-vesicular compartment at the cis-side of the Golgi apparatus. *J Cell Biol*. 107:1643-53.
- Shin, H.W., N. Morinaga, M. Noda, and K. Nakayama. 2004. BIG2, a guanine nucleotide exchange factor for ADP-ribosylation factors: its localization to recycling endosomes and implication in the endosome integrity. *Mol Biol Cell*. 15:5283-94.
- Silletta, M.G., A. Colanzi, R. Weigert, M. Di Girolamo, I. Santone, G. Fiucci, A. Mironov, M.A. De Matteis, A. Luini, and D. Corda. 1999. Role of brefeldin A-dependent ADP-ribosylation in the control of intracellular membrane transport. *Mol Cell Biochem*. 193:43-51.
- Sohn, K., L. Orci, M. Ravazzola, M. Amherdt, M. Bremser, F. Lottspeich, K. Fiedler, J.B. Helms, and F.T. Wieland. 1996. A major transmembrane protein of Golgi-derived COPI-coated vesicles involved in coatamer binding. *J Cell Biol*. 135:1239-48.
- Springer, S., E. Chen, R. Duden, M. Marzioch, A. Rowley, S. Hamamoto, S. Merchant, and R. Schekman. 2000. The p24 proteins are not essential for vesicular transport in *Saccharomyces cerevisiae*. *Proc Natl Acad Sci U S A*.
- Stagg, S.M., P. LaPointe, A. Razvi, C. Gurkan, C.S. Potter, B. Carragher, and W.E. Balch. 2008. Structural basis for cargo regulation of COPII coat assembly. *Cell*. 134:474-84.
- Stamnes, M.A., M.W. Craighead, M.H. Hoe, N. Lampen, S. Geromanos, P. Tempst, and J.E. Rothman. 1995. An integral membrane component of coatamer-coated transport vesicles defines a family of proteins involved in budding. *Proc Natl Acad Sci U S A*. 92:8011-8015.
- Strating, J.R.P.M., and G.J.M. Martens. 2009. The p24 family and selective transport processes at the ER-Golgi interface. *Biol Cell*. 101:495-509.
- Sutton, R.B., D. Fasshauer, R. Jahn, and A.T. Brunger. 1998. Crystal structure of a SNARE complex involved in synaptic exocytosis at 2.4[thinsp]Å resolution. *Nature*. 395:347-353.
- Tang, B.L., Y. Wang, Y.S. Ong, and W. Hong. 2005. COPII and exit from the endoplasmic reticulum. *Biochim Biophys Acta*. 1744:293-303.
- Tisdale, E.J., and M.R. Jackson. 1998. Rab2 Protein Enhances Coatamer Recruitment to Pre-Golgi Intermediates. *J Biol Chem*. 273:17269-77.
- Urbani, L., and R.D. Simoni. 1990. Cholesterol and vesicular stomatitis virus G protein take separate routes from the endoplasmic reticulum to the plasma membrane. *J Biol Chem*. 265:1919-1923.
- Volpicelli-Daley, L.A., Y. Li, C.J. Zhang, and R.A. Kahn. 2005. Isoform-selective Effects of the Depletion of Arfs1-5 on Membrane Traffic. *Mol Biol Cell*.
- Ward, T.H., R.S. Polishchuk, S. Caplan, K. Hirschberg, and J. Lippincott-Schwartz. 2001. Maintenance of Golgi structure and function depends on the integrity of ER export. *J Cell Biol*. 155:557-70.

- Waters, M.G., D.O. Clary, and J.E. Rothman. 1992. A novel 115-kD peripheral membrane protein is required for intercisternal transport in the Golgi stack. *J Cell Biol.* 118:1015-26.
- Weber, T., B.V. Zemelman, J.A. McNew, B. Westermann, M. Gmachl, F. Parlati, T.H. Sollner, and J.E. Rothman. 1998. SNAREpins: minimal machinery for membrane fusion. *Cell.* 92:759-72.
- Weigert, R., M.G. Silletta, S. Spano, G. Turacchio, C. Cericola, A. Colanzi, S. Senatore, R. Mancini, E.V. Polishchuk, M. Salmona, F. Facchiano, K.N. Burger, A. Mironov, A. Luini, and D. Corda. 1999. CtBP/BARS induces fission of Golgi membranes by acylating lysophosphatidic acid. *Nature.* 402:429-33.
- Yan, J.P., M.E. Colon, L.A. Beebe, and P. Melançon. 1994. Isolation and characterization of mutant CHO cell lines with compartment-specific resistance to brefeldin A. *J Cell Biol.* 126:65-75.
- Yang, J.S., S.Y. Lee, M. Gao, S. Bourgoïn, P.A. Randazzo, R.T. Premont, and V.W. Hsu. 2002. ARFGAP1 promotes the formation of COPI vesicles, suggesting function as a component of the coat. *J Cell Biol.* 159:69-78.
- Yoshida, Y., K. Suzuki, A. Yamamoto, N. Sakai, M. Bando, K. Tanimoto, Y. Yamaguchi, T. Sakaguchi, H. Akhter, G. Fujii, S.-i. Yoshimura, S. Ogata, M. Sohda, Y. Misumi, and N. Nakamura. 2008. YIPF5 and YIF1A recycle between the ER and the Golgi apparatus and are involved in the maintenance of the Golgi structure. *Exp Cell Research.* 314:3427-3443.
- Zeghouf, M., B. Guibert, J.C. Zeeh, and J. Cherfils. 2005. Arf, Sec7 and Brefeldin A: a model towards the therapeutic inhibition of guanine nucleotide-exchange factors. *Biochem Soc Trans.* 33:1265-8.
- Zhang, C., A.G. Rosenwald, M.C. Willingham, S. Skuntz, J. Clark, and R.A. Kahn. 1994. Expression of a dominant allele of human ARF1 inhibits membrane traffic *in vivo*. *J. Cell Biol.* 124:289-300.
- Zhao, L., J.B. Helms, B. Brugger, C. Harter, B. Martoglio, R. Graf, J. Brunner, and F.T. Wieland. 1997. Direct and GTP-dependent interaction of ADP ribosylation factor 1 with coatamer subunit beta. *Proc Natl Acad Sci U S A.* 94:4418-23.
- Zhao, L., J.B. Helms, J. Brunner, and F.T. Wieland. 1999. GTP-dependent binding of ADP-ribosylation factor to coatamer in close proximity to the binding site for dilysine retrieval motifs and p23. *J Biol Chem.* 274:14198-203.
- Zhao, X., A. Claude, J. Chun, D.J. Shields, J.F. Presley, and P. Melançon. 2006. GBF1, a cis-Golgi and VTCs-localized ARF-GEF, is implicated in ER-to-Golgi protein traffic. *J Cell Sci.* 119:3743-53.
- Zhao, X., T.K. Lasell, and P. Melançon. 2002. Localization of large ADP-ribosylation factor-guanine nucleotide exchange factors to different Golgi compartments: evidence for distinct functions in protein traffic. *Mol Biol Cell.* 13:119-33.